The Specialist Committee on Water Quality and Cavitation

Final Report and Recommendations to the 23rd ITTC

1. MEMBERSHIP AND MEETINGS

1.1. Membership

The membership of the Specialist Committee on Water Quality and Cavitation was:

- Professor Mehmet Atlar, (Secretary) Dept. of Marine Technology, University of Newcastle upon Tyne, Newcastle upon Tyne, United Kingdom
- Dr. Michael Billet (Chairman), Applied Research Laboratory, The Pennsylvania State University, State College, Pennsylvania, U.S.A.
- Dr. Laurence Briançon-Marjollet, Bassin d'Essais des Carènes, Val de Reuil, France
- Professor Steven Ceccio, Mechanical Engineering Department, University of Michigan, Ann Arbor, Michigan, U.S.A.
- Dr. Young-Gi Kim, Shipbuilding & Plant Research Institute, Samsung Heavy Industries Co., Ltd., Daeduk Science Town, Taejon, Korea (Resigned)
- Mr. Akira Oshima, Ship & Ocean Engineering Laboratory, Nagasaki Research and Development Center, Nagasaki, Japan
- Mrs. Elena Semionicheva, Krylov Shipbuilding Research Institute, St. Petersburg, Russian Federation
- Dr. In-Heang Song, Samsung Shipbuilding Model Basin, Samsung Heavy Industries Co. Ltd., Taejon, Korea

Due to a change in jobs, Dr. Young-Gi Kim was unable to continue his Committee membership and was replaced by Dr. In-Heang Song from the same organization.

1.2. Meetings

Four formal meetings of the Specialist Committee on Water Quality and Cavitation were held as follows:

Newcastle upon Tyne, United Kingdom, April 6-7, 2000, hosted by Professor Mehmet Atlar, Department of Marine Technology, University of Newcastle. This meeting was held in conjunction with the 50th Anniversary Conference of the University of Newcastle upon Tyne's Cavitation Tunnel, April 3-5, 2000, Newcastle upon Tyne, United Kingdom.

Val de Reuil, France, September 15-16, 2000, hosted by Dr. Laurence Briancon-Marjollet, Bassin d'Essais des Carenes. This meeting was held in conjunction with the 23rd Symposium on Naval Hydrodynamics, September 17-22, 2000, Basin d'Essais des Carenes, Val de Reuil, France.

Pasadena, California, USA, June 23-24, 2001, hosted by Professor Steven Ceccio, University of Michigan and held at the California Institute of Technology. This meeting

was held in conjunction with CAV2001, June 20-23, 2001, California Institute of Technology, Pasadena, California, USA.

London, United Kingdom, December 6-7, 2001, hosted by Dr. Michael Billet, Applied Research Laboratory, The Pennsylvania State University and Professor Mehmet Atlar, Department of Marine Technology, University of Newcastle. This meeting was held at the Royal Institution of Naval Architects, London, United Kingdom.

2. RECOMMENDATIONS OF THE 22ND ITTC

1. Review the development and recommend guidelines for the water quality measurements and conditions to minimize scale effects in cavitation.

2. Review the techniques and procedures for controlling and adjusting water quality characteristics in cavitation facilities.

3. Review the development of new extrapolation methods for cavitation inception data with regard to water quality parameters.

4. Carry out a study of flow mechanisms and related physical parameters that affect cavitation intermittence and instability including off-design conditions.

3. INTRODUCTION

The point of cavitation inception is conventionally defined as the flow conditions when cavitation is "first observed." Cavitation inception is inherently a statistical process, which involves the presence of cavitation nuclei (microbubble), in a specific local transient pressure field reduction for a necessary time period. Hence, probabilistic nature of bubble, capture, growth and collapse dictates that the inception process is always intermittent.

The frequency of discreet cavitation events generally increases continuously with reduction in the cavitation number. Consequently, different observers may "call inception" differently, depending on their ability to detect the initial cavitation events. Traditionally, singular cavitation events were not sensed, and thus the historical definition of cavitation inception occurred at operating conditions only after steady and repeatable cavitation events can be detected. Different definitions of cavitation inception can lead to difficulty in the interpretation of cavitation inception data and can make comparison between independent data sets problematic.

Thus, cavitation inception can be more precisely defined as the explosive growth of bubbles occurring at a specific rate, independent of the detection method.

The results of experiments conducted by members of the International Towing Tank Conference (ITTC) have provided impetus for attempts to quantify a relationship between cavitation nuclei, pressure field and cavitation inception (Lindgren & Johnsson, 1966; Johnsson, 1969; Acosta & Parkin, 1974). As a direct result, many definitive experiments were conducted that clearly demonstrate the specific role of viscous effects (Arakeri & Acosta, 1973; Van der Meulen, 1976) and free stream nuclei (Kuiper, 1981; Gates & Billet, 1980; Katz, 1981) on cavitation inception.

Cavitation studies have been reported in every International Towing Tank Conference proceedings since the 1966 experiments. However, the Cavitation Committee reports of the 20th ITTC (1993) and the 21st ITTC (1996) clearly define the importance of water quality on the propeller cavitation inception process. Water quality has been traditionally defined in terms of dissolved air content level; however, most researchers now define it in terms of liquid tension and/or nuclei number distribution.

In order to correlate water quality measurements with both visual and acoustic incep-

tion for several types of propeller cavitation, members of the 20th ITTC Cavitation Committee participated in tests at the Grand Tunnel Hydrodynamic (GTH) of the Bassin d'Essais des Carenes. The GTH offered a unique opportunity to correlate propeller leading-edge sheet, bubble and tip vortex cavitation inception with water quality data as determined by microbubbles (liquid tension), and microbubble number (event-rate). The results shown in Figure 3.1 clearly demonstrate a dependency of cavitation inception for each propeller cavitation type on liquid tension. Liquid tension T1 represents a 'zero' liquid tension case – weak water having many microbubbles. Liquid tension T4 represents a high value – very strong water having very few microbubbles.

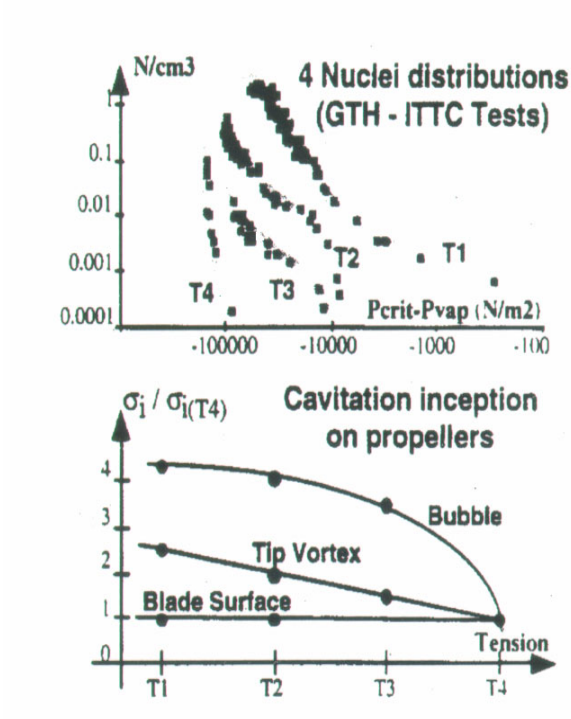

Figure 3.1 Nuclei distributions generated in the GTH and their influence on the cavitation inception value of the three 34-cm diameter propellers (20th ITTC, 1993).

The natural nuclei distribution of any cavitation facility depends upon the flow history and operating conditions. To quantify this effect, propeller cavitation inception tests were conducted in the Italian Navy Cavitation Tunnel (CEIMM tunnel). Cavitation nuclei measurements were made using a Centerbody Venturi that was similar to the one used in the GTH tests. These results are reported in the 21st ITTC Cavitation Committee Report and are summarized in Figure 3.2. These tests clearly show a need to account for water quality effects in propeller cavitation inception tests.

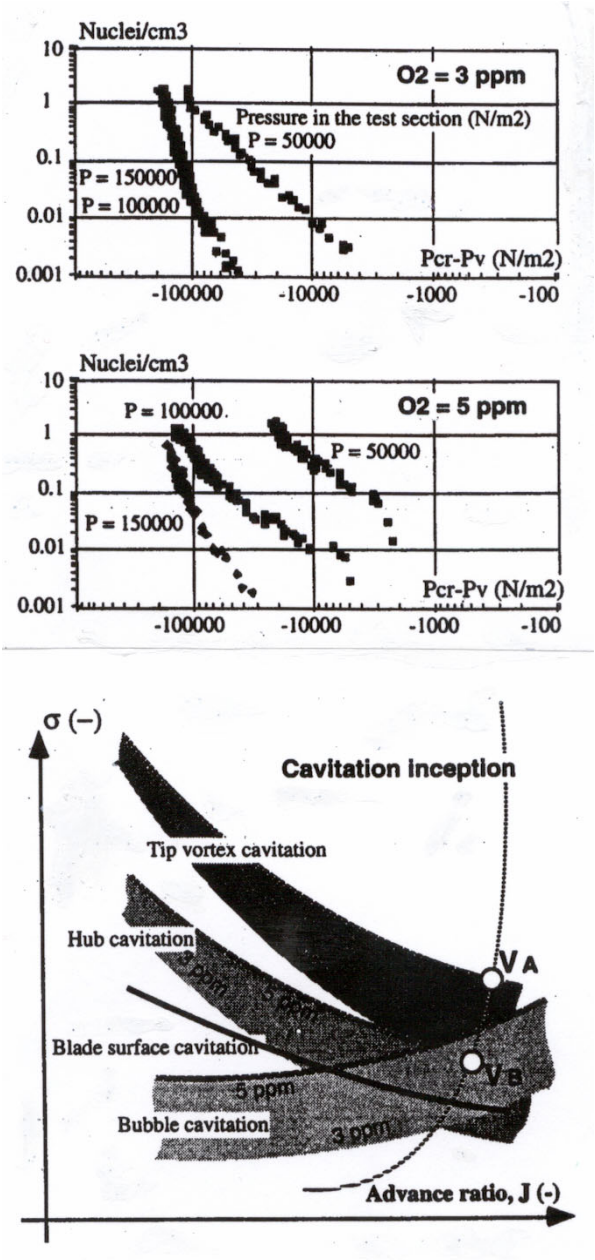

Figure 3.2 Influence of the water quality on the cavitation inception bucket (21st ITTC, 1996).

Understanding the role of water quality is very important for determining not only cavitation inception index, but also scale effects

for testing propellers. Minimizing the liquid tension and maximizing the number of critical nuclei is a general method to reduce water quality scale effects. However, in most testing, the control of water quality is not always possible. Propeller cavitation inception testing procedures used by various institutes are discussed in Section 4. Section 5 summarizes the various methods of defining water quality and presents measurements data.

Cavitation inception is commonly described by the cavitation number expressed as

$$\sigma_i = \frac{P - P_v}{\frac{1}{2}\rho V^2}, \qquad (1)$$

where P and V are the reference pressure and velocity, respectively, P_v is the vapor pressure at the bulk temperature of the liquid and ρ is the mass density of the liquid. The 'classical' theory for scaling vaporous cavitation inception states that σ = constant. This implies that when scaling from one flow state to another, not only are the characteristics of the flow field and its boundaries remaining geometrically and kinematically similar but also cavitation occurs when the local pressure is the liquid vapor pressure. However, real flows often do not obey this classical theory and departures are so-called "scale effects". Experimental results clearly show that in most cases, the cavitation inception index can be greater or less than the minimum pressure coefficient. One example of scale effects can be noted from the 'standard' cavitation tests conducted at many facilities for the ITTC.

In general, this study and several others resulted in scale effects being divided into two general types as follows:

Viscous Effects: Scale effects that act on the flow outside the cavitation bubble, which influence the local pressure in the liquid flow:

1. Flow field changes due to variations in Reynolds number, Froude number, and Mach number including steady and turbulent pressure fluctuations.
2. Departures from exact geometric similarity such as those due to roughness and finite manufacturing tolerances.

Bubble Dynamic Effects: Scale effects that act on the bubble growth process, which cause the liquid pressure at the bubble interface to depart from the equilibrium vapor pressure corresponding to the bulk temperature of the liquid:

1. Time effects due to bubble dynamics
2. Heat transfer effects
3. Surface tension effects
4. Transport of noncondensible gas
5. Liquid tension, i.e., a specific microbubble size and number density.

The focus of this specialist committee is on these bubble dynamic effects and on how to relate these to water quality. The fundaments of bubble dynamics as related to water quality effects are presented in Section 6. Also, several recent experiments are discussed.

As most organizations attempt in some manner to reduce water quality effects, the reality is that the natural nuclei spectrum of any cavitation facility depends upon the flow history. This means that for all facilities the natural spectrum will depend on the hydrodynamic conditions such as dissolved air content, pressure level and velocity, and the transit time of the tunnel circuit. As a consequence, the natural spectrum will be different for each condition/facility. Thus, extrapolation methods are utilized with cavitation inception measurements to correct for water quality effects and some of these are discussed in Section 7 of this report. Most of these methods attempt to correct the cavitation inception index to a value of having zero liquid tension, i.e., minimum water quality effects.

Finally, the committee has provided some recommendations for testing propellers,

measuring water quality and correlation/scaling of cavitation inception.

4. SUMMARY OF PROPELLER CAVITATION TESTING PROCEDURES

In order to determine how propeller-testing facilities measure cavitation inception and account for water quality scale effects, the committee conducted a survey of 18 large-scale test facilities. We received 16 responses to our survey. The questions were:

- What type of facility if used?
- How are the cavitation number and propeller advance ratio defined?
- How is cavitation inception defined?
- How is a point on the propeller performance curve determined?
- How is cavitation described?
- How are water quality conditions established prior to testing?
- How is cavitation scaling performed?
- How is water quality measured?
- How often is water quality measured?
- What is the basis for correlation between model and full scale?
- How is full-scale cavitation inception determined?

The main results are summarized in the following Table 4.1:

Table 4.1 Results of Propeller Cavitation Testing Survey.

A. Type of facility Used For Propeller Cavitation Inception Tests:	
open-jet type cavitation tunnel	**1**
closed-jet type cavitation tunnel	**16**
free-surface cavitation tunnel	**1**
depressurized towing tank	**1**
B. Determination of Propeller Inception Curves	
B.1. Definition of Cavitation Number:	**A variety of velocity and pressure measurements are used to define σ;**
	Both inflow speed and propeller tip speed are used;
	Pressures in the blade plane and upstream are used
B.2. Definition of Propeller Advance Ratio:	**A variety of velocity measurements are used to define J**
	Both inflow speed and propeller tip speed are used
B.3. Definition of Cavitation Inception:	**Video (4); Visual (11); Acoustic (5)**
B.4. Method used to obtain one point on a Propeller Cavitation Inception Curve:	**Some keep RPM constant and vary Pressure (4);**
	Some keep pressure constant and vary RPM (9); **Both RPM and Pressure Variation (2).**

B.5. How cavitation inception is called for specific kinds of cavitation:	
Tip vortex:	**1st Appearance (2); #blades (1); Attached TVC (3); Intermittancy Criteria (4)**
Hub vortex:	**1st Appearance (3); Attached HVC (1); Intermittancy Criteria (4)**
Bubble:	**1st Appearance (6); Intermittancy Criteria (4)**
Partial sheet:	**1st Appearance (4); 0.5 to 2 mm length at LE (4); desinence (1)**
B.6. Establishment of water quality conditions prior to cavitation inception testing:	**Air/Oxygen Content (16); Nuclei Dist. (5)*; Liquid Tension (1 + 1*)*rarely**
C. Instrumentation and Techniques for Controlling Water Quality	
C.1. Facility Characteristics	**Resorber (3); Degassser (14); Nuclei Injection (5); Electrolysis (1)**
C.2. Measurement of oxygen and/or gas content	**Oxygen Content (8); Gas Content (5); Both (3); None (0)**
C.3. Measuring devices used to monitor oxygen and/or gas content	**Van Slyke Device (7); DO Meter (9)**
C.4. Frequency of measurement	**Routinely (6); Before Testing (10); After Testing (4); With water change-out (1)**
C.5. Nuclei content measured	**No (7); Yes (2); no response (7)**
C.6. Frequency of nuclei measurements	**Routinely (0); With Investigative Purpose (6)**
C.7. Method of nuclei measurement	**PDA (2); Light Scattering (2); Holography (1); Venturi (2); Acoustic (1); CCD Camera (1)**
C.8. Determination of liquid tension	**No (7); Yes (3)**
D. Cavitation Scaling	
D.1. Testing procedures used to minimize scale factors	**Water Quality SE (7); Viscous SE (13)**
D.2. Scaling is applied to which types of cavitation	**Sheet (5); Bubble (4); TVC (12); HVC (8); None (2)**
D.3. Description of scaling methods for water quality effects	**Gas Content Regulation (5); Critical Pressure (1); Other (1); None (3); No Response (6)**
D.4. Description of scaling methods for flow fields	**FS Wake (5); Roughness application (1); Other (3); None (3); No Reply (4)**
D.5. What is the basis for correlation between model and full scale?	**Full Scale Correlation (9); Model Scale Exper. (5); Analysis (2); Combination (2)**
E. Method to Determine Full-Scale Propeller Cavitation Inception	**Visual (7); Acoustic (11); Vibration (1); Video/Photo (6)**

From the survey, it appears that the main method used to control water quality scale effects is through the control of the dissolved gas content to indirectly influence the nuclei population during testing. The nuclei content or critical tension of the freestream is not generally controlled or measured. It also appears that cavitation inception is defined in many different ways. The definition depends not only on the type of cavitation but also on the method used to detect inception. Explicit scaling for water quality is not generally performed.

5. TECHNIQUES FOR THE MEASUREMENT AND CONTROL OF WATER QUALITY

5.1. Introduction

To continue the work of the last Propulsion Committee, the Committee reviewed the techniques and procedures used by different research facilities to control and/or measure water quality. Then, based on these data, a brief description and bibliography is given on specific apparatus used to determine water quality.

An analysis of different measurement techniques is presented in order to emphasize the non-unique relationship between oxygen content or dissolved gas content and nuclei content. This is a unique problem for each facility that attempts to control water quality. Finally, a review of measuring techniques used at sea is provided and some results are given.

5.2. Questionnaire

In order to evaluate the cavitation tests conditions used by different facilities and the standard apparatus they use to measure water quality, a short questionnaire was sent to 20 organizations and 17 replies were returned. The questions were as follows:

- Do you modify oxygen or air content during tests?
- What is the standard oxygen or air content level for cavitation tests?
- Do you use the same content for noise measurements?
- Do you measure nuclei content in the tunnel?
- How do you measure it?
- Where do you measure it?
- What are the standard nuclei content for cavitation tests?
- Do you measure water surface tension?
- If yes, how do you measure it?
- Do you measure viscosity of water tunnel?
- If yes, how do you measure it?
- Could you describe your process to increase or decrease the oxygen or gas content level in the tunnel?

The main results are summarized in Table 5.1. The results of the last ITTC questionnaire are included for comparison.

It appears that all the participants to the questionnaire measure oxygen and/or gas level during inception tests. Just one or two facilities measure free nuclei and only for special tests. There is no universal rule concerning the level of oxygen or gas content. Each facility has its own procedure correlated to full-scale measurements. It is obvious that even with the same oxygen content, two different facilities will often yield two different inception sets of data for the same model. There is only one facility, which is able to control independently dissolved gas and free nuclei.

Table 5.1 Summary of Survey.

Type of Contents Measured		22nd ITTC
O_2	59 %	
Total gas	18 %	
Both O_2 and total gas	23%	
Standard Level		
30%-40% of saturation at atmospheric pressure	53%	Low 36 %
60%-80% of saturation at atmospheric pressure	18%	Medium 40%
90%-100% of saturation at atmospheric pressure	12%	High 16%
100% of saturation at test pressure	12%	
Undersaturation at test Pressure	6%	
Nuclei		
For specific tests	35 %	12%
Once	18 %	
Never	47%	
Surface Tension		
Once	29 %	
Never	71 %	
Viscosity		
Once	12 %	
Never	88 %	

Some facilities (29%) change the oxygen/gas content by running the tunnel with low pressure for reducing the air content level. Other facilities (12%) use a procedure similar to the first one but with the tunnel half full. Almost half of the facilities (53%) used a specific degassing device. An amount of water is by-passed from the tunnel into a device with a free surface and in which the pressure can be decreased or increased. Sometimes, the sampled water is spread into droplets in order to increase the exchange surface.

One facility uses a specific procedure consisting of running the tunnel at low speed, at low or high pressure level depending on if the oxygen content is decreased or increased and injecting a large number of nuclei in the tunnel. The exchange surface area is very large and thus it is not time consuming to reach a low or high air content. All the bubbles are then separated from the water in a large tank.

To increase the oxygen content, some facilities (29%) add some fresh water. Another facility uses its deaeration device with high pressure or puts air into the tunnel and then runs it with high pressure.

For noise measurements, one facility conducted tests with over-saturated water, four facilities use a gas content higher than 60%, and two facilities decrease the level used for standard cavitation measurements to avoid signal attenuation due to the presence of bubbles.

Surface tension and viscosity are not routinely measured. Viscosity is calculated using temperature of the water.

The following table summarizes the nuclei measuring system utilized in water tunnels:

Table 5.2 Summary of Measuring Methods.

Light scattering method	17 %
Microscope	5 %
PDA	22 %
Holography	17 %
Acoustic method	11 %
Venturi	28 %

Note: Several facilities have compared two or three different devices.

5.3. Measuring Device Description

5.3.1. What Do We Need to Measure?

Water quality is related to the distribution and concentration of small free stream gas bubbles. These bubbles are uniquely related to the dissolved air content level and the flow history for each facility. The aim of all tests is to be able to determine and to extrapolate cavitation inception data taking into account water quality effects.

The critical pressure P_c of a bubble is the maximum pressure value at which this bubble begins to explode. This physical characteristic of the bubble is based on equilibrium equation of a bubble :

$$P_v + P_{g0} = P_{\infty 0} + \frac{2S}{R_0} \tag{5.1}$$

where R_0 is the equilibrium radius under pressure in the fluid $P_{\infty 0}$, P_v is the vapor pressure of the fluid and S is the surface tension of the fluid.

When the pressure in the flow is decreased, the radius of the nuclei increases and the critical pressure corresponds to the pressure below which the bubble can not have an equilibrium radius. It can be written as a function of initial characteristics of the bubble as:

$$P_c = P_m - P_v = \sqrt{\frac{32S^2}{27R_0^3 P_{g0}}} \tag{5.2}$$

Fluids have a nuclei distribution which include different radii and thus different critical pressures. Knowing the critical pressure distribution of the nuclei allows us to know directly how the fluid will cavitate to a specific pressure distribution.

Hence, the liquid will cavitate when the bubbles it contains grows explosively. That means cavitation inception for any specific type (bubble, vortex) will take place when the local pressure in the fluid will be equal to the critical pressure of the many nuclei in the liquid. It is very important to know the minimum pressure in the flow field because it can be extrapolated to a large scale. So, when making cavitation tests, the results indicate when the minimum pressure in the flow is equal to the liquid critical pressure (i.e., tension is equal to zero). Knowing the critical pressure of the liquid, the minimum pressure of the flow is known. The correction factor on σ can be expressed as:

$$\Delta\sigma = \frac{P_c - P_v}{\frac{1}{2}\rho V^2} \tag{5.3}$$

The tensile strength of a fluid is defined as a specific value of the critical pressure. For example it can be the maximum critical pressure of nuclei contained in a fluid or it can be the critical pressure value corresponding to a given value of nuclei concentration. The liquid tension parameter is strongly related to the way the cavitation inception is defined, measured and extrapolated during the experiment.

Different nuclei distribution's can yield approximately similar critical pressure values, so it is important to know both the critical pressure and nuclei concentration.

Gindroz & Billet (1998) found that specific nuclei concentrations must be used for each type of cavitation. For example 0.0001 nuclei per cm^3 for bubble inception at 10 m/s on the water tunnel and 0.01 nuclei per cm^3 for tip vortex inception. In addition, there will be an effect on the propeller cavitation type between model and full scale.

Gowing & Shen (2001) used a cavitation susceptibility meter (Venturi type) to measure tensile strength of water in tunnels, lakes and oceans. They used an inception criterion of an event-rate range from 3 to 10 events per minute. The results (nuclei radius) are used to define a correction factor for tip vortex extrapolation between model and full scale. It must be noted that they used the same criterion for model and full scale based on the events measured by the same apparatus.

5.3.2. How do we measure?

The undissolved gas content on free nuclei can be measured with two families of devices. Some devices measure the nuclei contained in the fluid. This can be accomplished by optical methods and acoustic methods. Others measure the cavitation response of a nucleus when subjected to a known pressure field. The devices are described below.

Oxygen Content

Dissolved oxygen content is usually measured with a device that uses a reaction between the dissolved oxygen and an electrode. Both immersion probe and membrane devices are used. Nuclei size and distribution are not measured.

Gas Content

The total gas content is measured with a Van Slyke device. A liquid sample is degassed in a closed apparatus and the volume of extracted gas is measured. By this way, both dissolved gas and the gas contributed from free bubbles are measured. Nuclei size and distribution are not measured.

Nuclei Size-Optical

Optical devices detect nuclei and measure the size of the microbubble directly through the collection of techniques are used:

- Optical microscopy.
- Micro-holography (Gates & Bacon, 1978; Yu et al., 1997; Gindroz et al., 1998).
- Light scattering method (Keller, 1972; Billet, 1986; Bongiovani et al., 1997).
- Phase Doppler Analyser PDA (Gowing, 1980; Tanger et al., 1989; Liu et al., 1998).

Optical methods can be used to directly measure the nuclei content in the free stream or in a by-pass stream of water. Each method has its own particular resolution, advantages, and limitations. Overall, optical methods can typically measure nuclei down to ~10 μm in diameter. Optical methods have difficulty in distinguishing between very small gas bubbles and solid particles.

Nuclei Size-Acoustic

The resonance frequency of a small bubble is related to its radius, and the local sound speed is related to the void fraction of the bubbles mixture. Thus, acoustic propagation can be used to determine nuclei distributions in the water. A review of the acoustic methods can be found in Young or Oldenziel (1982). These techniques have been used for at-sea measurements.

Nuclei Size-Critical Pressure

The Cavitation Susceptibility Meter (CSM) is an hydraulic apparatus (Venturi tube) in which pressure at the throat is varied by varying flow rate. An acoustic sensor or an optical sensor is used to count cavitation events that occur in the throat. The number of nuclei, which explodes, is plotted against a variation in the throat pressure. That way, the critical pressure cumulative distribution of the nuclei in the fluid can be determined. The nuclei size can be related to the pressure of the throat via static equilibrium equation.

Different types of CSM have been tested:

- A simple throat with an optical detection (d'Agostino & Acosta, 1991), with an acoustic detection (Lecoffre, 1979; El Goff, 1983; Gowing, 1999, 2001).
- A throat with a centerbody (Gindroz & Billet, 1998; Gowing, 1999; Pham et al., 1995, 1997).
- A throat with a vortical flow (Keller, 1981).

Comparison between several nuclei measurment methods is given by Gindroz & Billet (1998), Friesch (2000) and ITTC (1990, 1996). Gowing (1999) compared the data given by two types of Venturi (a simple one and a Centerbody Venturi) and found a good agreement between both devices.

Billet (1986) compared microbubble distribution measured with the light-scattering system and with holography. Good agreement has been found between these two devices.

The comparison between nuclei radius data obtained by optical methods and CSM measurements still give some discrepancies. The radius of nuclei calculated from critical pressure measured by Venturi is often smaller than the radius directly measured by optical method.

5.4. Nuclei and Air Content of Facilities

Different facilities (Gindroz et al., 1996) are characterized by different nuclei distributions, corresponding to the hydrodynamic configuration of each facility. The nuclei spectrum is influenced by the time history of the water through the facility. The use of a de-aerator to remove air and a resorber to dissolve the small nuclei can change significantly the spectrum. As a consequence, the natural spectra will not only be different in each cavitation facility, but it will also strongly depend on the facility operating condition.

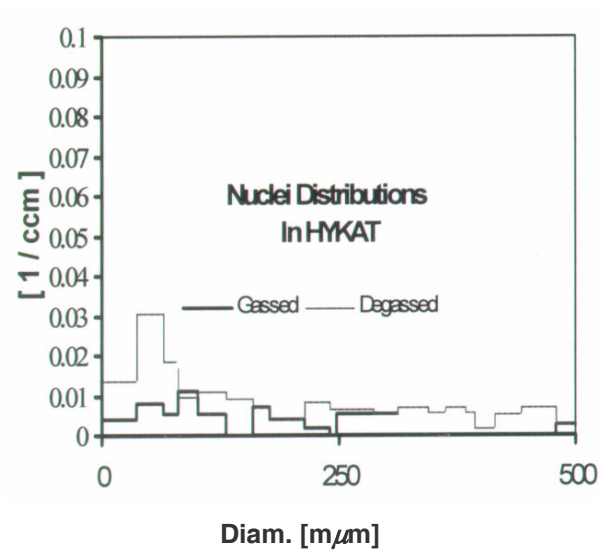

Figure 5.1 Nuclei distribution in HYKAT for two oxygen contents measured with an optical method (PDA) (Friesch, 2000).

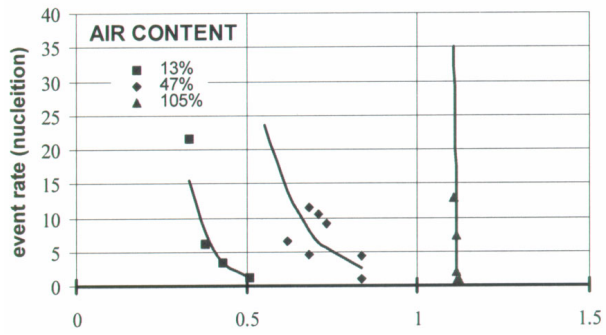

Figure 5.2 Nuclei distribution in 12 inch water tunnel at DTMB measured with CSM from Gowing (2001).

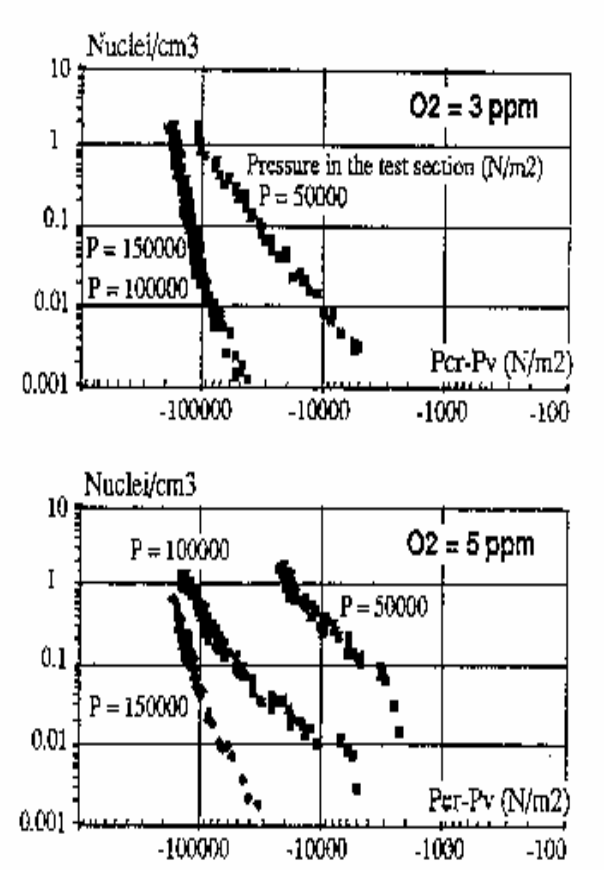

Figure 5.3 Nuclei distribution in the CEIMM facility with a Centerbody Venturi (21st ITTC, 1996).

Three different facilities are illustrated in Figures 5.1, 5.2, and 5.3. When the oxygen content is low, the mean diameter of nuclei decrease. This results in an increase in the tensile strength of the water (see for example CEIMM). This is the reason why many stud-

ies have found a good correlation between oxygen content and cavitation inception.

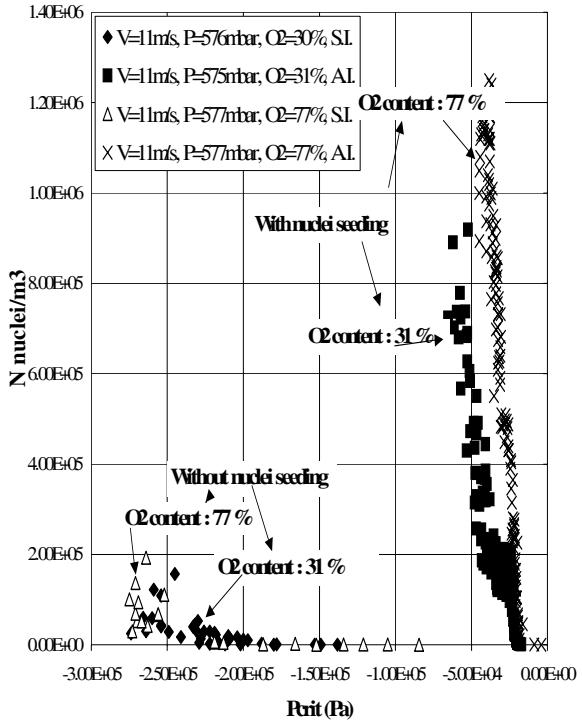

Figure 5.4 Nuclei distribution in the GTH as measured by Centerbody Venturi showing the Influence of the nuclei seeding and Oxygen content.

Only one facility (GTH) can control separately the oxygen content and the nuclei distribution (Frechou et al., 2000). Thus, the effect of the oxygen content and the free nuclei on cavitation can be studied as shown in Figure 5.4 (Gindroz et al., 1998; Gowing et al., 1995; Briançon-Marjollet et al., 1996).

It can also be seen that for the same oxygen content and the same facility, when the test pressure is varied, the nuclei distribution changes (Gindroz & Matera, 1996). This means that during cavitation tests the critical pressure will be different between higher and lower tunnel pressures (Briançon-Marjollet et al., 1996). For example using the data from CEIMM and an oxygen content of 5 ppm, the correction factor $\Delta\sigma$ associated with the cavitation parameter is noted in Table 5.3:

Table 5.3 Correction Due to Liquid Tension.

P_c-P_v (Pa)	V (m/s)	σ	$\Delta\sigma$	Precentage Change
-10^4	6 m/s	5.4	0.55	10
-2.10^3	6 m/s	2.6	0.11	4.2

Moreover, two facilities with the same air content can have very different nuclei distributions. Indeed for a large cavitation tunnel, the residence time is much higher than for medium size or small size and this leads to a better dissolution of nuclei in the water. As a consequence, the number and size of nuclei is much lower for the same oxygen content, see for example Figure 5.5. In this case, there is 92% of oxygen content in the HYKAT and 51% in the medium size tunnel. However, the nuclei distribution is higher in the medium size tunnel than in HYKAT which is a very large tunnel.

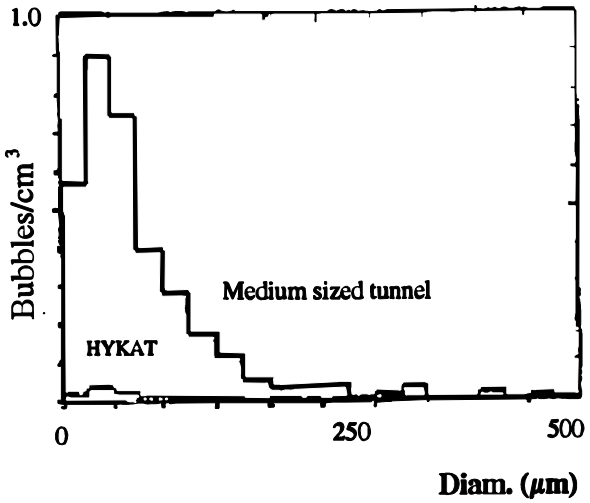

Figure 5.5 Nuclei Distribution in HYKAT and Medium Sized Tunnel Measured with an Optical Method (PDA) (Friesch, 2000).

From all of these examples illustrating different types of facilities (except the Depressurized Towing Tank in which the air content is always at saturation value at the pressure used) it is obvious that correlations based on air content level only is not sufficient.

5.5. Nuclei content for sea water

Measurements of nuclei distribution of sea water have been made by many investigators. Some results are shown in Figures 5.6 and 5.7. Holography, light-scattering device, acoustic device and Venturi have been used to make at sea measurements.

The most recent investigation shows the evolution of the nuclei distribution with depth. It shows that when the depth increases, the size and number of nuclei decrease. The oxygen content level related to atmospheric pressure does not vary by depth. The results obtained during full-scale tests are plotted in the Figure 5.7 for cumulative nuclei pressure distribution and in Figure 5.8 for oxygen content. In this graph, oxygen content is related to local pressure.

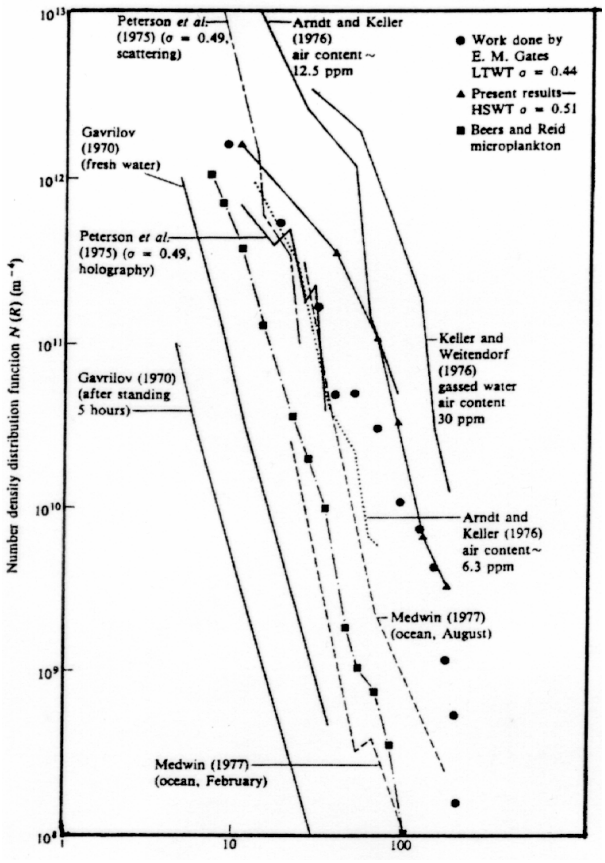

Figure 5.6 Nuclei distributions from various sources. (Katz, 1978).

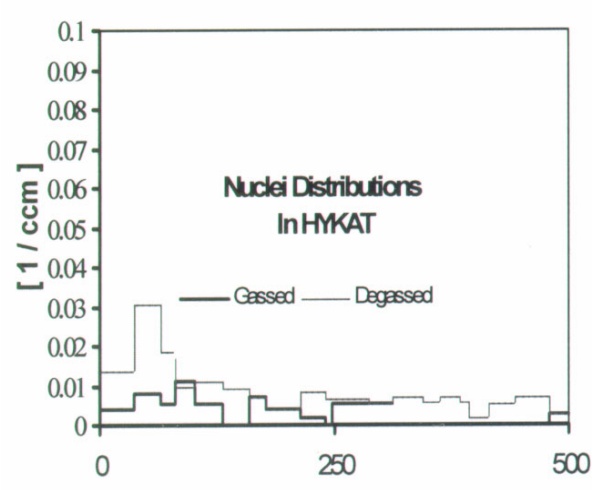

Figure 5.7 Cumulative nuclei distribution versus depth (Venturi device). Data from North Atlantic (Bassin d'Essais des Carènes).

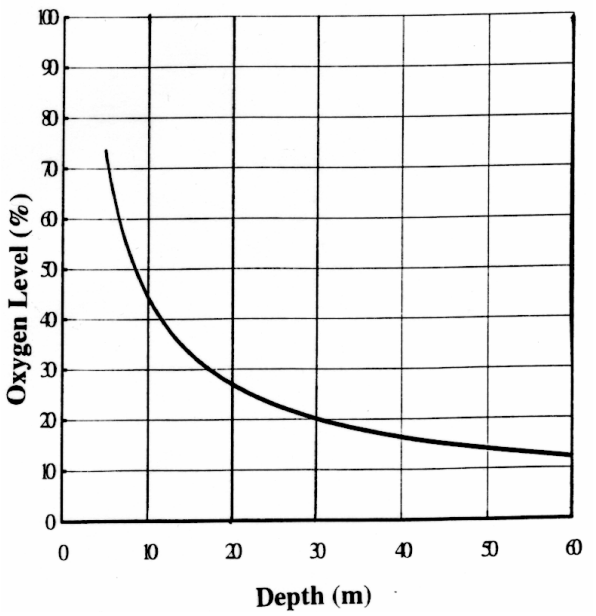

Figure 5.8 Oxygen content level related to local pressure versus depth. Data from North Atlantic (Bassin d'Essais des Carènes).

Gowing and Shen (2001) made nuclei distribution measurements both in a lake and in the ocean. These measurements were done with a standard Venturi device. Figure 5.9 summarizes these measurements for different depths at Lake Pend Oreille.

A comparison between Lake Pend Oreille data and ocean data are given in Table 5.4.

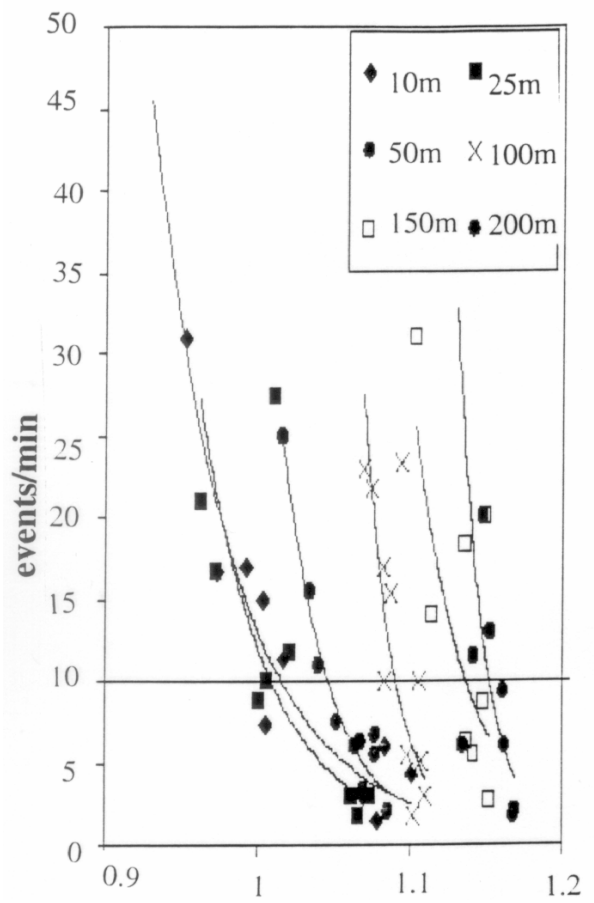

Figure 5.9 Cumulative nuclei distribution versus depth at Lake Pend Oreille (using a Venturi device) (Gowing & Shen, 2001).

Table 5.4 Comparison between Lake and Oceans. Radius of active nuclei for cavitation inception (Gowing & Shen, 2001).

model water tests		full-scale test locations				
Pend Oreille		Exuma Sound 1983				
1985		Depth (m)	Sta. 3	Sta. 4	Sta. 5	Sta. 6
Depth (m)	R_0 (μm)	25	0.53	0.64	0.94	0.65
10	1.57	75	0.62	0.57	0.67	1.13
25	1.21	North Atlantic Ocean 1985				
1986		Depth (m)	Sta. 3	Sta. 4	Sta. 5	Sta. 7	Sta. 10
Depth (m)	R_0 (μm)	25	0.77	1.07	0.49	0.58	0.72
10	1.30	50	0.54	0.46	0.30	0.46	0.40
25	0.70	100	0.30	0.32	0.28	0.25	0.27
1987		Pacific Ocean 1986				
Depth (m)	R_0 (μm)	Depth (m)	Sta. 1		Sta. 2	
10	1.22	62	0.41		0.49	
25	1.23					

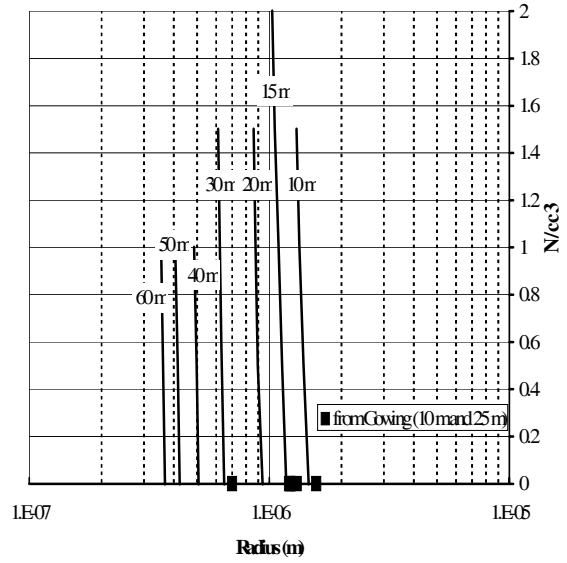

Figure 5.10 Cumulative nuclei distribution versus depth (Venturi device). Data is from North Atlantic (Bassin d'Essais des Carènes) and is compared with data from Gowing & Shen (2001).

A comparison between measuring devices is shown in Figures 5.10 and 5.11. Data from Gindroz & Gowing (2001) with the CSM compared quite well. Figure 5.11 shows the envelope from all the curves from O'Hern et al. (1985) and the data from the Bassin d'Essais de Carènes. It can be noted that the CSM give radii smaller than those obtained by acoustic and optic device.

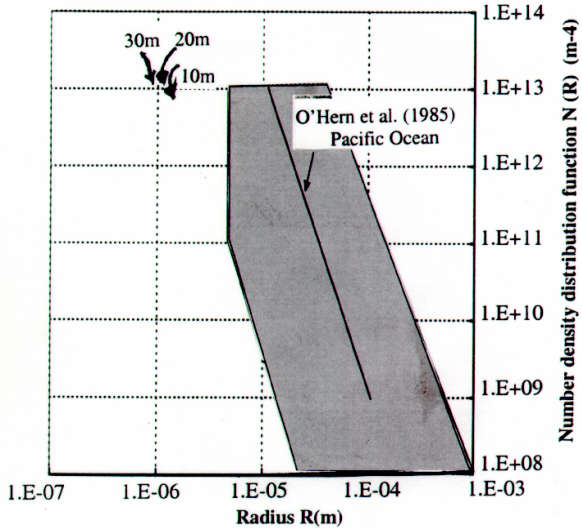

Figure 5.11 Comparison between the envelope of data from figure and Bassin d'Essais des Carènes data with center body Venturi.

6. FLOW MECHANISMS AND WATER QUALITY

6.1. Bubble Dynamics and Water Quality Effects

The various factors that cause scale effects and influence cavitation inception can be ascertained by employing the Rayleight-Plesset equation. This equation describes the growth of a "typical" cavitation bubble and can be written as

$$\rho\left(R\ddot{R}+\frac{3}{2}\dot{R}^2\right)=P_g-\frac{2S}{R}-\frac{4\mu\dot{R}}{R}-[C_P(t)+\sigma+C_T(t)]\frac{1}{2}\rho V^2$$

where

$$C_P(t)=\frac{P(t)-P}{\frac{1}{2}\rho V^2}$$

and

$$C_T(t)=\frac{P_v(T)-P_v(Tr(t))}{\frac{1}{2}\rho V^2} \tag{6.1}$$

Thus $C_P(t)$ is the time varying pressure coefficient which describes the variation of the liquid pressure outside of the bubble. The thermodynamic coefficient (C_T) describes the effect of heat transfer on the vapor pressure in the bubble. The term P_g is the partial pressure of gas inside the bubble and the term $2S/R$ is the tension of the bubble. Multiplying equation (6.1) by a time interval (dt), integrating over a time interval which is typical of a cavitation process, and solving for σ yields

$$\sigma=-\overline{C}_P+\frac{\overline{P}_g}{\frac{1}{2}\rho V^2}-\frac{\frac{2\overline{S}}{R}}{\frac{1}{2}\rho V^2}-\phi-\overline{C}_T \tag{6.2}$$

where, ϕ is a bubble dynamic parameter. The bars denote averages over the time interval. In the absence of significant dynamic effects, equation (6.2) reduces to an equilibrium equation given as

$$\sigma=-\overline{C}_P+\frac{\overline{P}_g-\frac{2\overline{S}}{R}}{\frac{1}{2}\rho V^2}-\overline{C}_T \tag{6.3}$$

It is important to note that the dynamic effects are only important during the initial acceleration of the bubble wall during cavitation inception (Holl, 1970). Referring to equation (6.3), it is noted that the terms P_g, $2S/R$, and C_T all cause bubble dynamic scale effects and the bubble tension term and thermodynamic coefficient will reduce the cavitation number at inception and the gas pressure in the bubble will increase the cavitation number at inception. Viscous scale effects are contained with the average pressure coefficient $\overline{C}_P$. This can be written as

$$-\overline{C}_P=-\overline{C}_{P_s}+\frac{\overline{\Delta P_T}}{\frac{1}{2}\rho V^2}+\frac{\overline{\Delta P_R}}{\frac{1}{2}\rho V^2}+\frac{\overline{\Delta P_U}}{\frac{1}{2}\rho V^2} \tag{6.4}$$

where $\overline{C}_{P_s}$ is the average local pressure in the absence of surface roughness $\overline{\Delta P_R}$, turbulence, $\overline{\Delta P_T}$ and flow unsteadiness $\overline{\Delta P_U}$.

Equation (6.3) provides some insight into scaling issued for water quality effects. The thermodynamic coefficient is only important in super-heated or cryogenic liquids (Holl & Korhauser, 1970). Viscous scale effects are in the term C_P which are assumed to be constant in this investigation. Thus, water quality effects on isolated bubbles (at cavitation inception) are represented as follows

$$\sigma=-C_{P_{\min}}+\frac{P_g-\frac{2S}{R}}{\frac{1}{2}\rho V^2}-C_T \tag{6.5}$$

First of all, as the velocities increase, both gas pressure and bubble tension terms become less important. For cases where there are many large bubbles, the surface tension term becomes small and cavitation inception occurs when the local pressure is vapor pressure. This condition is typically called "zero liquid tension". However, if the dissolved air content is high, then cavitation inception can occur above the flow minimum pressure coefficient.

This type of cavitation is nonvaporous and is given the term pseudo or gaseous cavitation. Pseudo cavitation occurs when a bubble merely expands due to a reduction in pressure with the mass of gas in the bubble essentially remaining constant. Gaseous cavitation occurs when a bubble grows in an oversaturated liquid due to the transport of gas across the interface. Correlations of non-vaporous cavitation inception data with equation (6.5) have been done by Holl, Arndt, and Billet (1972). Finally, if the majority or all of the microbubbles present are very small and few, a significant liquid tension exists and cavitation inception will occur at pressures significantly below the pressure corresponding to the flow minimum pressure coefficient.

In general, the criteria for cavitation inception testing have been: 1) high velocity, 2) moderate dissolved air content level, and 3) sufficient number of microbubbles in the range of 10 to 100 μm in diameter. This can be noted in the example given in Figure 6.1 using equation (6.5) over a range of dissolved air content levels, microbubble diameters, and velocity. This example assumes bubble cavitation inception on a body having minimum pressure coefficient of –1.5, which is constant over the velocity range.

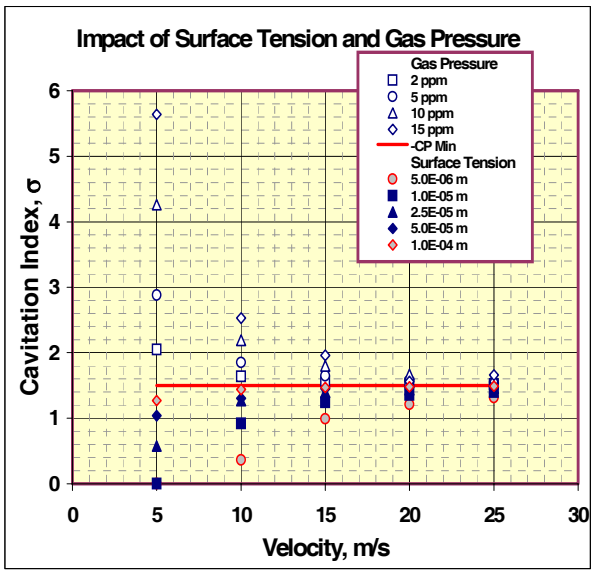

Figure 6.1 Impact of surface tension and gas pressure.

Perhaps, the best propeller experiment that provides insight into liquid tension effects (P_g–$2S/R$) remains the 1992 joint Bassin d'Essais des Carènes and ITTC Cavitation Committee test. These tests summarized in Figure 6.1 clearly demonstrate the reduction in cavitation inception index for an increase in liquid tension.

In this experiment, the nuclei distribution was determined from a Center body Venturi as described in Section 5.3. Varying the flow rate through the Venturi, which changes the reference pressure, and counting of the corresponding cavitation events accomplish this. The relationship between the Venturi critical pressure and critical radius comes from static equilibrium and is given by

$$R_c = \frac{-3\Gamma - I}{3\Gamma}\left(\frac{2S}{(P_m - P_v)_c}\right) \qquad (6.6)$$

Again, using bubble equilibrium, this critical tension ($P_m - P_v$) that gives R_c can be related to initial tunnel conditions thus giving R_0. This can be expressed as:

$$P_c = P_m - P_v = \sqrt{\frac{32S^3}{27R_0^3 P_{g_0}}} \qquad (6.7)$$

where P_{g_0} can be expressed in terms of Henry's Law

$$P_g = K\alpha\beta$$

where α is the dissolved air content and β the Henry's law constant. More information on these measurements can be found in Gindroz & Briançon-Marjollet (1992).

From these microbubble distributions, the critical liquid tension can be defined as

$$T_c = P_v - P_c \qquad (6.8)$$

where P_v is the vapor pressure, and P_c is the critical microbubble pressure of the largest microbubble chosen at a specific density.

This liquid tension value can be utilized to correct for bubble dynamic effects. The cavitation number can be written as

$$\sigma = \frac{P - P_v}{\frac{1}{2}\rho V^2} + \frac{P_g - 2S/R}{\frac{1}{2}\rho V^2}$$
$$= \frac{P - P_v}{\frac{1}{2}\rho V^2} + \frac{P_c}{\frac{1}{2}\rho V^2}$$
$$= \frac{P - P_v}{\frac{1}{2}\rho V^2} - \frac{P_m - P_v}{\frac{1}{2}\rho V^2} \qquad (6.9)$$

These tests clearly show the sensitivity of cavitation inception to liquid tension/nuclei distribution. It was found to be different for each type of propeller cavitation. For an extreme range of liquid tension, blade surface cavitation had a maximum of 3% reduction in cavitation index, tip vortex cavitation had a maximum of 59% reduction in cavitation index, and bubble cavitaiton had a maximum of 76% reduction in cavitation index for increasing liquid tension.

Additional analysis of these data provided a methodology to correct for this scale effect and addresses the critical issue of intermittency. In the absence of viscous effects, intermittency is solely due to the number of critical microbubbles or "event rate".

6.2. Cavitation Event-Rate, Intermittency and Liquid Tension

It must be appreciated that cavitation inception is a deceptively difficult condition to define. Defining the exact conditions under which cavitation will first occur is like trying to answer the question – when does a pot of water boil? Water can be heard to 'boil' before the usual observation can be made. It is not surprising that this is true of cavitation where the acoustic detection occurs before visual. Most experimental observations of cavitation inception are based on first appearance of cavitation bubbles; however, this is not always the case in propeller cavitation where bubbles repeated in a specific location can be the criteria. It is clear that there is not a sharply defined condition of inception since the criteria are largely subjective and the phenomenon is sensitive to a number of factors.

A recent experiment conducted at ARL Penn State attempted to define cavitation inception by event rate. A comparison of cavitation inception criteria can be noted by comparing visual to acoustic tip vortex inception on a stationary hydrofoil. Visual was done by a strobe light used for propeller cavitation. Acoustic event counting was done with a near-field high frequency sensor and signature post-processing. The results are shown in Figure 6.2. One result from this test shows that in this case the visual call (a few per second) could be actually a greater number of events.

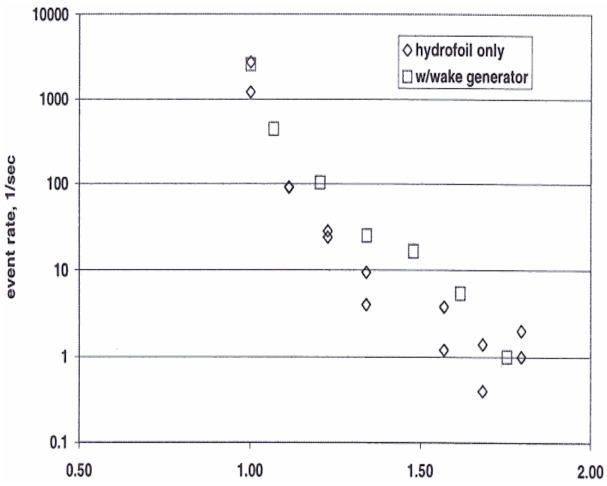

Figure 6.2 Event rate versus cavitation number.

Figure 6.2 also shows a significant change in event rate slope. This trend is expected for any cavitation inception data; however, the slopes will vary. Little change in the cavitation inception index occurs between 10 to 1000 events per second. However, below 10 events per second a significant change in cavitation index occurs to a value of 1 event per second. This is due not only to the nuclei distribution of the larger microbubbles in the tunnel but also background noise levels. The larger microbubbles are few and the probability of inception is small. Near visual inception there exists many more microbubbles that can cavitate in this case.

Thus, the liquid tension (T) corresponding to inception must be related to an event rate (nuclei distribution). Let S^* be the cross section of the cavitation flow, C^* the absolute velocity of the flow through this section, and let $N = R$ in this function $\Rightarrow N = \text{fcn}(Pv - P_{cr})$ or $N = F$ (nuclei size) be the number of activated nuclei per unit volume. The nuclei concentration leading to an event rate ζ can be defined as follows:

$$\zeta\,(\text{events/s}) = N(\text{nb/m}^3)S^*(\text{m}^2)C^*(\text{m/s})$$

$$\therefore \quad \text{N} = \zeta/(S^*C^*) \qquad (6.10)$$

Then, considering that cavitation generally corresponds to an event rate of one per second, the corresponding number of activated nuclei N^* and the corresponding tension T^* will be

$$N^* = 1/(S^*C^*)$$

$$T^* = \text{f}\,(N) \qquad (6.11)$$

This relationship between liquid tension/event rate and cavitation inception is discussed in detail in the Cavitation Committee Report of the 21st ITTC. However, a brief summary of bubble and tip vortex caitation inception is included here.

Figure 6.3 shows the evolution of the cavitation inception index with water tension for the 'bubble' and 'tip vortex' propeller cases. There is a linear relationship for the bubble propeller but there exists a more complicated relationship for the 'tip vortex' propeller. The characteristic cross-section of the cavitation flow differs between the two cases and is shown in Figure 6.4. As can be noted, the propeller surface cross-section area where cavitation can occur is significantly larger than the cross-sectional area for the tip vortex. In addition, the pressure field for each type is different which leads to a 'selection' of the available nuclei distribution.

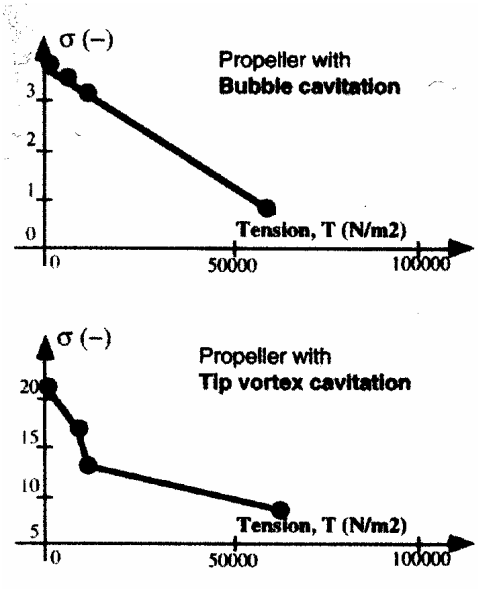

Figure 6.3 Evolution of the cavitation inception value with the water tension as determined from the nuclei distributions for the "bubble" and the "tip vortex" propeller cases (21st ITTC).

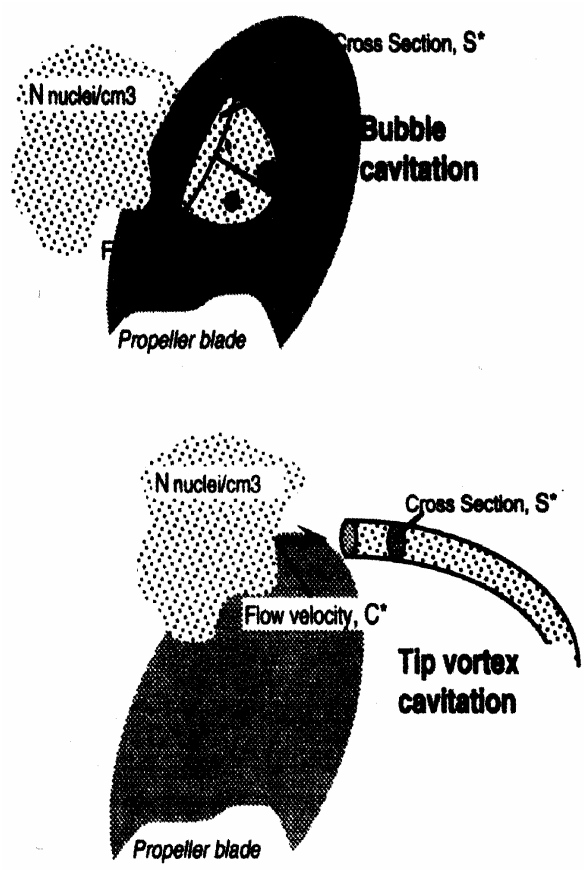

Figure 6.4 Cross section of the cavitating flow for bubble and tip vortex cavitation.

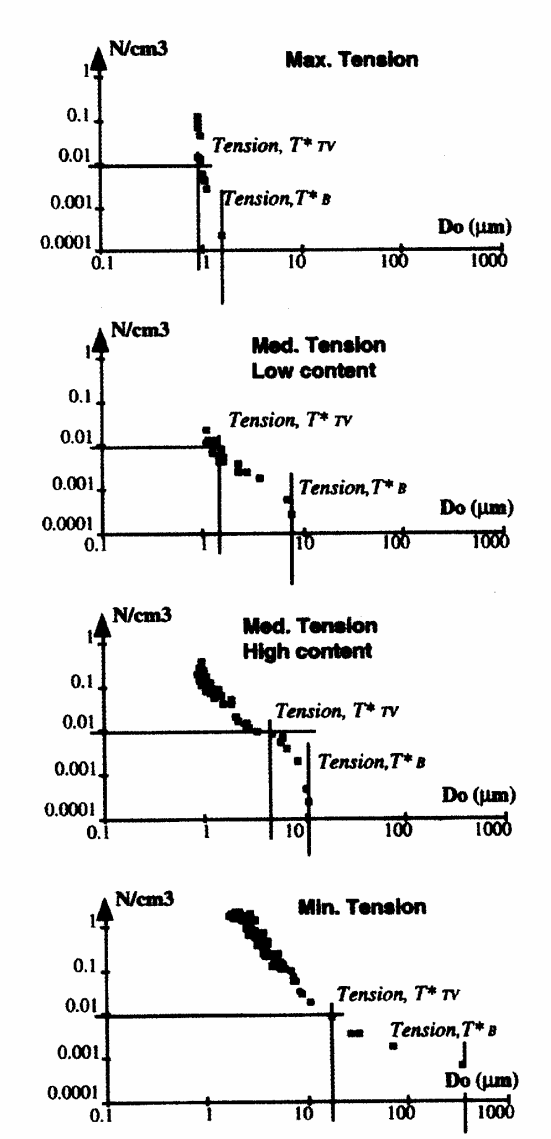

Figure 6.5 Nuclei distributions and corresponding characteristic tensions, T^*_B and T^*_{TV} (21st ITTC).

Analysis of the cavitation inception data in reference to Equation (6.11), indicates that the nuclei content differs by two orders of magnitude between the bubble and tip vortex cases (order of magnitude of 0.0001 nuclei/cm3 for tip vortex cavitation). Figure 6.5 shows the difference in tension values between bubble cavitation inception, T^*_B and tip vortex inception, T^*_{TV}, for the four nuclei distributions generated. Using this "event rate" approach, the cavitation inception data for σ_i correlate well with the tension value T^* as shown in Figure 6.6.

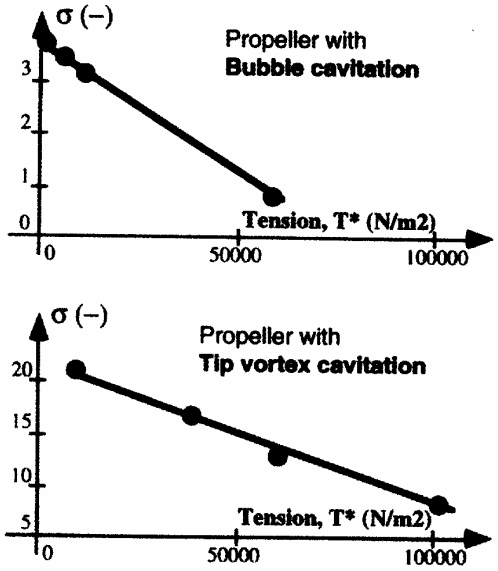

Figure 6.6 Influence of the tension T^* on cavitation inception (21st ITTC).

In summary, the liquid tension is also related to the event rate intermittency. The presence of many nuclei in the critical size range (determined by the pressure field) increases the event rate near inception and decreases intermittency. Also, the corresponding liquid tension depends upon an event rate. It is also important to note that increasing the velocity and the cavitation area (increase in size) will decrease water quality effects.

6.3. Numerical Analysis

The rate of discreet cavitation events can be predicted using numerical methods. Farrell (2000) developed an Eulerian/Lagrangian computation procedure for the prediction of cavitation inception by event rate. As noted previously, the event rate is governed by the number and distribution of nuclei, the instantaneous pressure field in the flow, the trajectory of the nuclei, and the bubble dynamics. The probability of a cavitation event $P(e)$, the principle result of his simulation, is equal to the number of nuclei which cavitate over the number of nuclei in the ensemble and can be expressed as

$$E = N^{*}A_c V_c P(e) \quad (6.12)$$

The threshold event rate can be quite larger than one, depending on the number of nuclei in the ensemble. For example, if one computes that one computational bubble among 800 will cavitate, then the threshold event rate would be 5000 per second for a typical axisymmetric body and measured nuclei distribution.

Detailed calculations were done on a "Schiebe" body and comparisons were made to Meyer (1989) and Kuhn de Chizelle et al. (1995). Simulated and experimental values of the cavitation inception number for various event rates are shown in Table 6.1 where the minimum pressure coefficient on the body is –0.78. Indeed these simulations show clearly that the reduction in cavitation number with increasing free-stream velocity is due to the changing nuclei distribution in the tunnel. In addition, typical event rates near inception are in the order of 1000 due to the large number present, but significantly decrease as velocity increases.

The filtering effect of headform pressure distribution significantly affects the probability of low-event-rate cavitation as the cavitation number approaches the minimum pressure coefficient. As a result, event rates for bubble cavitation inception are typically of several orders of magnitude. The probability of cavitation events at this condition appears to be principally driven by pressure fluctuations in the flow. Thus the vortex forms of cavitation would be more susceptible to low event-rate cavitation than surface forms where the minimum pressure occurs near the flow boundary and boundary layer pressure fluctuations are less.

The interaction of discreet nuclei with a concentrated vortical flow has also been studied numerically. Hsiao & Pauly (1999) performed numerical calculations to examine the process by which individual nuclei are captured by a tip vortex. A RANS simulation of the non-cavitating flow was created, and the dynamics of individual nuclei were examined as they convected into the core of the tip vortex. Most studies of this type will employ "one-way" coupling of the flow to the dynamics of the bubble. The motion and growth of the bubbles are assumed not to influence the flow field. More complex bubble flow interactions are also being examined for relatively simple flows. Hsiao & Chahine (2001) examine bubble vortex interactions using combined Navier-Stokes simulations of the flow with a Chimera moving grid scheme to capture bubble dynamics. Iyer et al. (2001) used direct numerical simulations to study the capture process of single nuclei. These studies can ultimately lead to the prediction of discreet cavitation event rates for a given description of the vortical flow field.

Table 6.1 Simulated and experimental values of the cavitation inception number for various event rates.

Free-stream Velocity (ft/sec)	Cavitation Index for visual inception	Event-rate via visual interrogation (sec^{-1})	Predicted cavitation index at visual event rate	Predicted cavitation index at 200 events per second
30	0.55	3638-7146	0.49-0.53	0.56
40	0.60	865-1507	0.53-0.55	0.52
50	0.56	734-1132	0.59-0.61	0.50
60	0.53	537-476	0.63-0.64	0.51

6.4. Experimental Results

Experimental research on the influence of gas on cavitation inception and dynamics over the past 20 years has been reviewed by Rood (1991) and Gindroz & Billet (1998). The experiments discussed in Gindroz & Billet were also discussed above. Recent work examining the physical processes responsible for water quality effect on cavitation inception have been limited. Nuclei effects on tip vortex inception have been extensively examined by researchers in France and Switzerland, and reviews of this effort can be found in Fruman (1994). The influence of dissolved gas in the inception and development of tip vortex cavitation was examined by Briançon-Marjollet & Merle (1996). They demonstrated how both free and dissolved gas content would influence the cavitation of a stationary elliptic planform hydrofoil along with the core diameter and dynamics of the vortex. While the size of the incident nuclei were not a free parameter of the study, it was shown that the dynamics and fragmentation of larger bubbles in the vortex can influence the noise the bubbles emit upon collapse. Such bubble dynamics can be influenced by the initial nuclei spectrum.

Kamiirisa (2001) showed how free and dissolved gas content could influence the noise spectrum emitted by cavitating propellers (with both leading edge and vortex cavitation). The noise emitted by propellers cavitating in both fresh and salt water for varying dissolved air contents was examined, and it was concluded that both free and dissolved air content has to be managed in fresh water testing to produce analogous nuclei content associated with the salt-water tests. This is consistent with the results of Ceccio et al. (1997) who showed that the nuclei content of artificial salt water was significantly lower than that of fresh water for similar dissolved air content.

Researchers at the Naval Surface Warfare Center and the University of Michigan are currently examining tip leakage vortex inception as it occurs on a ducted propulsor (Ceccio et al., 2001 and 2002b). The flow field vortex is examined with both three component Laser Doppler Velocimetry (LDV) measurements and two-dimensional Particle Imaging Velocimetry (PIV). The goal of this study is to understand how the average and instantaneous flow field of the leakage vortex changes with Reynolds number, and how flow field parameters are related to vortex cavitation inception. Figure 6.7 shows a schematic diagram of the ducted rotor under study.

Measured flow quantities of the leakage vortex include the instantaneous and average vortex size, circulation, and position. These quantities will be related to the measured inception curves. Preliminary measurements of the rotor inception confirm the influence of water quality on the inception characteristics.

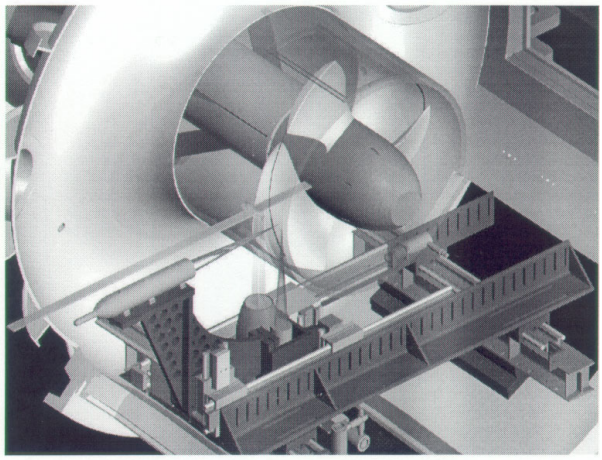

Figure 6.7 Schematic Diagram of the 5206 Rotor mounted in the NSWC-CD 36 Inch Water Tunnel. The propeller duct is shown. An optical window has been placed in the duct for access of the PIV light sheet and LDV laser beams. The PIV camera and LDV transmitting and receiving optics are placed in watertight compartments within the open jet test section.

Figure 6.8 shows various measurements of the free-stream susceptibility in the 36-inch water tunnel measured with a cavitation susceptibility. Note that this water tunnel is equipped with a resorber. It is clear that the

susceptibility is a function of both the dissolved gas content and the tunnel static pressure. In turn, variation in free-stream susceptibility will lead to variation in the called inception values. Figure 6.9 shows the visually called cavitation inception value for vortex cavitation favoring susceptibility at a constant flow Reynolds number.

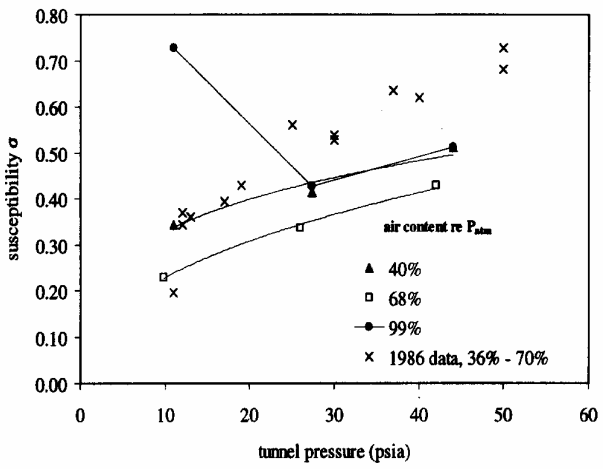

Figure 6.8 Susceptibility of the free-stream flow in the 36 inch Water Tunnel at the US Naval Surface Warfare Center. The susceptibility is a function of both dissolved gas content and free-stream pressure.

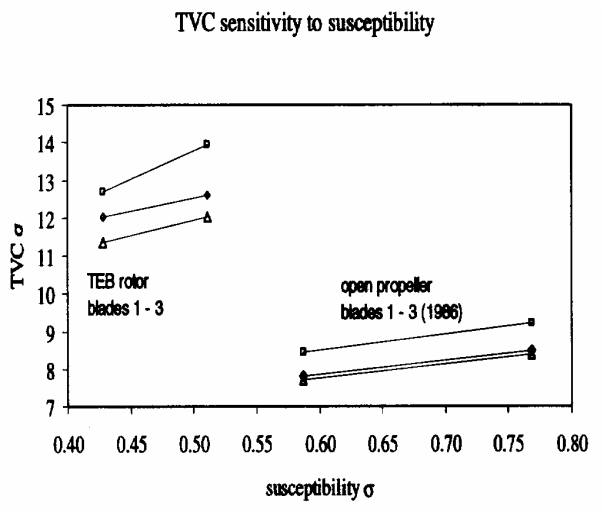

Figure 6.9 Inception number of tip vortex cavitation as a function of measured susceptibility for a constant flow Reynolds number.

Semionicheva & Startsev (2001) examined scale effects on various multi-point two-dimensional section profiles. Experimentally observed cavitation patterns were shown to vary with Reynolds number in the region where traveling bubble cavitation occurred on the hydrofoils. These scale effects were associated with the inferred test facility nuclei characteristics as well as a velocity effect that resulted from residence time of individual nuclei in the region of high tension.

Korkut & Atlar (2001) examined the importance of free-stream turbulence on inception testing of propellers. They showed that an increase in the ingested free-stream turbulence level can be equivalent to the application of surface roughness for boundary layer tripping. These results may have implication for water quality scale effects as well since strong free-stream turbulence can alter the incoming nuclei distribution.

7. REVIEW OF EXTRAPOLATION METHODS TO CORRECT WATER QUALITY

7.1. Introduction

In this section, a review of recent scaling methods, post 21st ITTC, for cavitation inception is presented in Section 7.2. The scaling equation proposed by Keller, (see e.g. Keller, 2001) is reviewed separately in Section 7.3, while Section 7.2 presents other recent extrapolation methods with a specific emphasis on the correction for water quality.

7.2. Methods to correct water quality

The issue of scaling for cavitation inception has been discussed at previous Cavitation and Propulsion Committees of the ITTC. Perhaps the most comprehensive and up to date discussion of the scaling with regards to the water quality was presented in the report of

the 21st ITTC Cavitation Committee (ITTC, 1996). This is particularly for the scaling of tip vortex cavitation inception, since its prediction heavily relies on model tests and hence requires application of scaling due to the understanding the complex flow field of the tip vortex. In this report, the scale effects on tip vortex cavitation inception are grouped into pressure field (lift, geometry, viscous (Reynolds number)) and bubble dynamics (water quality).

With regards to the above categories, the Reynolds number scaling of the tip vortex cavitation, is expressed by the well-known relationship based on the McCormick's classical work with a series of model tests on tip vortex cavitation inception with different planforms, model sizes and aspect ratio of foils, McCormick (1962). This relationship indicates that cavitation inception index; σ_i increases with a power of Reynolds number $Re^{0.35}$. A more recent experimental study reported in Fruman et al. (1991) reveals that σ_i is to increase $Re^{0.4}$. Since different values of the Reynolds number power have been in use at various testing facilities, this expression, assuming that the effects of water quality and lift magnitude are held constant, is presented in the following form:

$$\sigma_i = (\text{const})\, Re^m \tag{7.1}$$

where the Reynolds number is based on a representative chord length. Some examples of recommended values for exponential factor m from different sources are given in a tabulated form in the Cavitation Committee report of 21st ITTC. The differences in these values are attributed to test facility differences, range of tested Reynolds number and variations of water quality.

The effect of the water quality scaling of tip vortex cavitation inception is initially done in investigations on fixed hydrofoils reported in Fruman (1994), Arndt & Maines (1994), Pauchet et al. (1994) and Fruman et al. (1995). The following expression for the critical cavitation number, σ_{cr} "corrected" for liquid tension effects is represented by

$$\sigma_{cr} = \sigma_{i0} - \frac{P_c - P_v}{\frac{1}{2}\rho V^2} \tag{7.2}$$

where σ_{i0} is idealized (free of tension effect) cavitation inception number. P_c is to be read at the reference velocity equal to 0, as the extrapolation of the measured static reference pressures, where the inception or desinence occur, plotted against $\frac{1}{2}\rho V Re^{0.4}$, for each angle of attack.

Later, based upon the experiments with a large elliptical planform of NACA 0020 foil section in the Grand Tunnel Hydrodynamique, Briançon-Marjollet & Merle (1996) also proposed a corrective term for the inception of tip vortex cavitation in order to account for the measured water quality which was characterized in terms of the oxygen and free stream nuclei content. Assuming that the inception occurs at the susceptibility pressure P_m of the water instead of the vapor pressure, they expressed this correction in the following form:

$$\sigma - \Delta\sigma = \frac{P - P_v}{\frac{1}{2}\rho V^2} - \frac{P_m - P_v}{\frac{1}{2}\rho V^2} \tag{7.3}$$

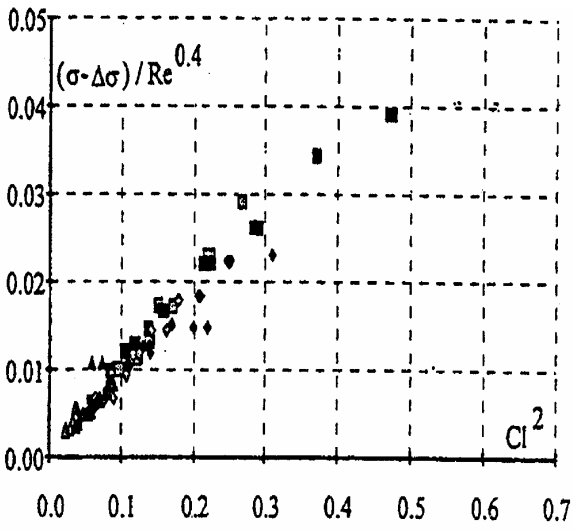

Figure 7.1 Corrected parameter at inception versus lift coefficient squared for tip vortex cavitation from elliptical planform of NACA 0020 foil section from Briançon-Marjollet & Merle (1996).

$$\sigma - \Delta\sigma = \frac{P - P_m}{\frac{1}{2}\rho V^2} \tag{7.4}$$

As shown in Figure 7.1, although the corrected cavitation parameter well correlated even those without nuclei injection, it was indicated that the main difficulty of this method would be the evaluation of P_m, which was measured using a Cavitation Susceptibility Meter (CSM) based on a Venturi, as a statistical value derived from a sample of several liters of water.

The effect of the water quality scaling of tip vortex and bubble cavitation inception on propellers proposed by Gindroz (1995) uses an "event rate" for the estimation of correction tension T^*. This approach, which takes into account the nuclei effects on cavitation inception, is a physically intuitive approach using a CSM to measure the cumulative nuclei concentrations over a range of tension for a few conditions of water quality, and the cavitation inception data for the model collected at the same time. The water quality conditions can be adjusted by changing the air content or pressure history. Based on the cavitation event rate, that defines inception, and an estimate of the water flow through cavitating area (S^*), nuclei concentration (N^*) is calculated which corresponded to the observed cavity event rate at inception. These events can be visual or acoustic. The tension (T^*) corresponding to the incipient nuclei concentration is determined from each of the CSM nuclei spectra, and the set of tension values are normalized by the dynamic pressure of the model test ($\frac{1}{2}\rho V^2$), V being the reference velocity. The model's cavitation inception indices (σ_i) are then compared to the normalized tensions (τ^*) to determine the sensitivity of the model inception to changes in water tension ($d\sigma_i/dT^*$). This value can then be used to correct the model's inception index (σ_i) to conditions of zero tension (σ_{i0}) or any other tension that the full-scale propeller may encounter, by the following expression:

$$\sigma_i = \sigma_{i0} - \frac{T^*}{\frac{1}{2}\rho V^2} \tag{7.5}$$

In deriving Equation 7.5, based upon the experimental analysis reported in Gindroz & Billet (1998), Gindroz & Billet (1994a and 1994b), Gindroz (1995) described a correction tension term T^* (actually a pressure term) which depends on activated number of nuclei (N^*) involving the particular cross section area of the cavity (S^*) and the absolute velocity of the flow (C^*) through this section, generally corresponding to an event rate of one per second, as in the following:

$$N^* = 1/(S^*C^*) \tag{7.6}$$

$$T^* = \mathrm{f}\,(N^*) \tag{7.7}$$

As shown in Figure 7.2, using this "event rate" approach, the cavitation inception data (σ_i) collected for the tip vortex and bubble cavitation are correlated well with T^* displaying a linear relationship, with the following slope:

$$d\sigma_i / dT^* = \frac{1}{\frac{1}{2}\rho V^2} \tag{7.8}$$

The equation of the lines in Figure 6.6 is represented by Equation 7.9 which relates cavitation inception to a normalized "event rate" tension:

$$\sigma_i = \sigma_{i0} - \tau^* \tag{7.9}$$

where, τ^* is normalized event rate tension given by

$$\tau^* = \frac{T^*}{\frac{1}{2}\rho V^2} \tag{7.10}$$

and

$\sigma_{i0} = \sigma_i$ value for zero tension (i.e. $T^* = 0$).

This methodology utilizes the nuclei density and the characteristic dimension of the propeller in its correlation (event rate to determine tension). This applies not only to model scale correlations but also to full scale predictions.

In a recent study, Shen et al. (2001) discussed the modifications of the scaling equation for tip vortex cavitation inception recommended by the 19th ITTC Cavitation Committee. The following equation was proposed:

$$\sigma_{if} \Big/ \sigma_{im} = K\left(\frac{Re_f}{Re_m}\right)^n \tag{7.11}$$

where subscripts "f" and "m" denote the full-scale and model respectively while *Re* is the Reynolds number based on the chord length and the resultant blade inflow velocity at 0.7 radius for a propeller. Exponential *n* and *K* are empirical factors, the latter to represent the nuclei effects and to assign appropriate values for *n* and *K*, there were no specific recommendations made by this Committee. Their discussion is based on experimental evidence that suggests the inception number approaches to a limiting value as the air content is systematically increased and the value of *K* is often set to 1 in many testing facilities. In practice it is assumed that if the model is tested at high air content, nuclei effect on cavitation inception are small. This assumption is not always justifiable based on the theoretical work performed by Ceccio & Brennen (1992) who demonstrated that it is the bubble size distribution and bubble size concentration and the fact that each facility has an unique relationship between dissolved air content and nuclei. They also emphasized an acoustic interpretation of inception for larger models, since the visual technique can hardly be applied to full-scale tests, which involve sound pressure level and frequency measurements that are affected by the bubble behavior as well as simple event rates. Based upon the above argument, Shen et al. (2001) suggested a modified scaling formula for tip vortex cavitation that also separates the viscous (Reynolds number) and nuclei (water quality) effects. The viscous effects determine the scale effect on the pressure field in which the bubbles respond, and the acoustic behavior of different size bubbles are then calculated in both of those pressure fields as outlined in the following.

Based on geometric and kinematics similarity, the theoretical analysis of the circulation, core size and pressure distribution of a trailing vortex present the relationship between the cavitation inception for the model and full-scale tip vortex, excluding the nuclei effects, as in the following form:

$$\sigma_{if} \Big/ \sigma_{im} = \frac{C_{P\min f}}{C_{P\min m}} = \left(\frac{Re_f}{Re_m}\right)^{0.4} \tag{7.12}$$

where subscripts f and m are associated with the full-scale and model and $C_{P\min}$ is the minimum pressure coefficient. The above scaling formula, which requires that boundary layers on model and full-scale are both turbulent, also agrees with Fruman's measurements.

Assumed (i.e., many nuclei) in the case that the effect of the gas bubbles is taken into account, the cavitation inception σ_i would not occur at $-C_{P\min}$ instead to occur later at $-(C_{P\min} + \Delta\sigma)$. It then follows:

$$\frac{\sigma_{if}}{\sigma_{im}} = \frac{\left(-C_{P\min f} - \Delta\sigma_f\right)}{\left(-C_{P\min m} - \Delta\sigma_m\right)} = G\left(\frac{Re_f}{Re_m}\right)^{0.4} \tag{7.13}$$

where

$$G = \frac{\left[\dfrac{1+\Delta\sigma_f}{-C_{P\min f}}\right]}{\left[\dfrac{1+\Delta\sigma_m}{-C_{P\min m}}\right]}. \tag{7.14}$$

Equation 7.13 is very similar to the form of law proposed in the 19th ITTC Cavitation Committee report (i.e. Equation 7.11) with a simple factor "*G*" which represents the effect of water quality on cavitation inception between the full-scale and model.

In order to calculate the *G* value, Shen et al. (2001) approximate the tip vortex field using the Burger's vortex model. In this prescribed vortex pressure field, the behavior of a

spherical bubble is described with an improved bubble dynamics model based on the Rayleigh-Plesset equation where the effect of slip velocity between the bubble and the carrying fluid, and the liquid compressibility are taken into account. The latter would be important when bubble-wall velocities become comparable with the sound of speed in the liquid as well as to take into account energy loss by acoustic emission. Furthermore, in the enhanced model, ambient pressure is taken to be an average of the pressure local to the bubble surface in order to avoid an unbounded bubble growth when the bubble is captured by the vortex line and hence to have a more realistic description of the bubble behavior. The motion of the bubble in the prescribed pressure field is described using Maxey's & Riley's (1983) equation adapted for a gas bubble based on various assumptions and simplifications, to study the bubble trajectory and its volume variation during bubble capture by the tip vortex. In relating the factor G to cavitation inception, they preferred an acoustic technique to define inception. Using the curve of maximum acoustic pressure versus cavitation number they obtained the rate of pressure change with the cavitation number, $-\mathrm{d}P/\mathrm{d}\sigma$ and the cavitation inception number was defined as the largest cavitation number for which $-\mathrm{d}P/\mathrm{d}\sigma >> 1$. With the developed model described above, Shen et al. (2001) performed numerical investigations to evaluate G, in representing the effect of nuclei on tip vortex cavitation inception, given by:

$$G = \left(\frac{\sigma_{if}}{\sigma_{im}}\right)\left(\frac{Re_m}{Re_f}\right)^{0.4} \qquad (7.15)$$

Figure 7.2 shows the values of G against the ratio of nuclei size between model and full scale (R_{0m}/R_{0f}) for varying initial bubble size, R_{0m} in the model tests. As notead, the value of G can be greater, equal or less than 1 depending on the relative effect of tensile strength of available gas bubbles between the model and full-scale.

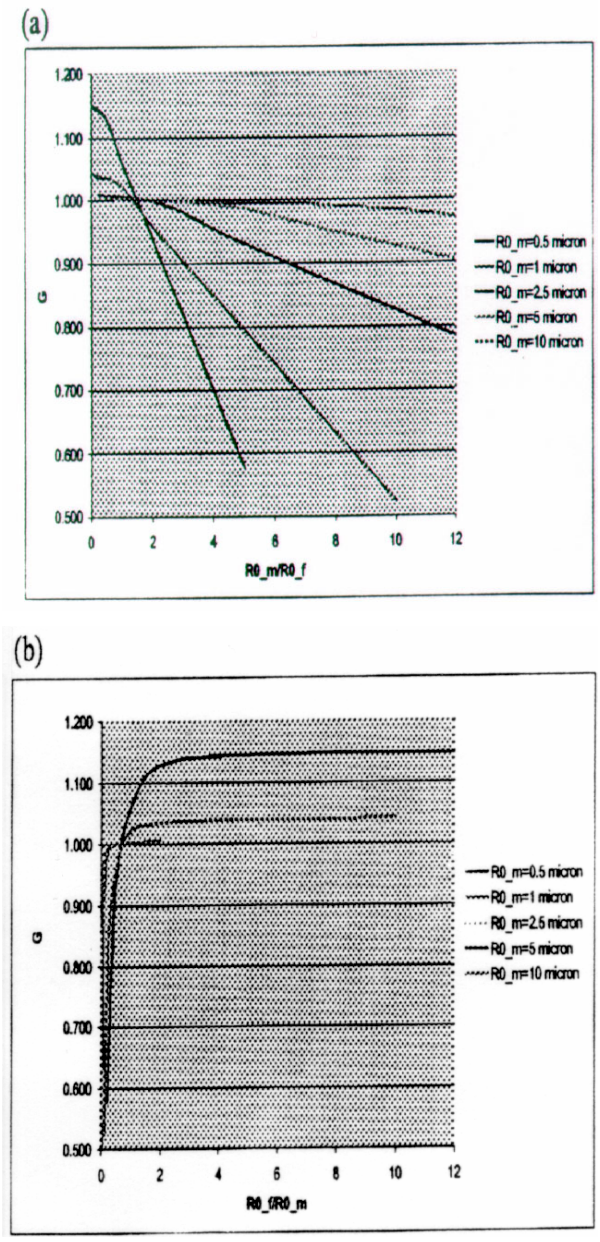

Figure 7.2 Curves of the nuclei parameter, G versus the ratio of the nuclei size between Model and full scale R_{0m}/R_{0f} for varying initial bubble size, R_{0m} in the model tests. (Shen et al., 2001).

As shown in Figure 7.2, for the same nuclei distribution between the model and full-scale (i.e. $R_{0m}= R_{0f}$), G is greater than 1.0, indicating that water quality exhibits stronger effect on the model than full-scale, particularly with small nuclei size. In order to have no nuclei effect between the model tests and full-scale observations (i.e. G=1.0), the initial bubble size in the model test must be slightly

greater than in the full scale ($R_{0m}>R_{0f}$). However if the initial bubble size in the model tests is much greater than in full-scale (i.e. $R_{0m} >> R_{0f}$), the effect of the water tensile strength at cavitation inception will be weaker in the model tests than in full scale observations resulting in $G < 1$. On the other hand if $R_{0m} << R_{0f}$, the effect of the tensile strength at cavitation inception will be relatively strong at model than in the full-scale, resulting in $G > 1$. In essence, the nuclei effect, which leads to deviation from the traditional scaling law, is increased as the bubble sizes at model sidediffer from full-scale.

In order to explore the effect of nuclei variations on tip vortex cavitation inception, Gowing & Shen (2001) applied the above described "**G**" factor approach for the scaling of hypothetical propeller tip vortex cavity in a lake and various locations in oceans. The nuclei size data used for this investigation were derived from the analysis of 3 years of water tensile strength data collected by the US Navy in Lake Pend Oreille, Bahama Islands, the Pacific Ocean along the US West Coast, and the North Atlantic Ocean, using a CSM. These tensile strength data were related to equivalent bubble size using the bubble stability equation to produce a spectrum of bubble concentration versus bubble size. The ratio of bubble sizes corresponding to a selected CSM cavitation rate (e.g., 10 per minute) in different water bodies (i.e., lake and ocean) was assumed to be the same as the bubble sizes in the incipient cavitating tip vortex. Furthermore, the bubble sizes responsible for the model-scale tip vortex cavitation inception were assumed to be the same as those for the selected rate measured in the model water body tests of the CSM.

The magnitude and variability of the nuclei related scaling effects were calculated for a hypothetical ¼-scale submarine propeller test run in the lake at different times and scaled to different full-scale ocean locations. The G factors were estimated for hypothetical model tests done in each of the 3 years lake data and the variance of the full-scale predictions were calculated for the above-mentioned locations in the ocean. Figure 7.3 shows the calculated "G" factor against the ratio of bubble sizes (R_{0m}/R_{0f}) for various initial bubble sizes in the lake.

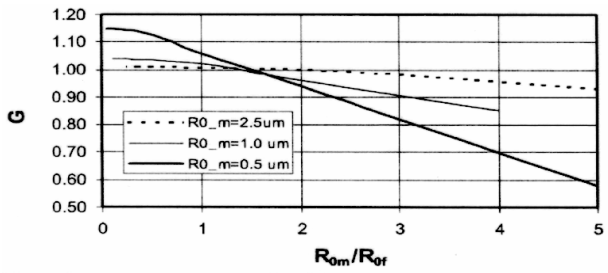

Figure 7.3 Nuclei parameter "G" for ¼-scale tip vortices, Gowing & Shen (2001).

As shown in Figure 7.3, the values of G depend on the scale factor, the ratio of the bubble sizes and the initial bubble size in the model tests. In general the scale effects become more severe for greater size ratios and smaller initial nuclei sizes in the model scale. Because no actual cavitation tests were performed during the nuclei measurements, Gowing & Shen assumed a model cavitation speed (20 knots) and two inception depths (10 m and 25 m), which were selected to correspond to the depths where nuclei data were collected in the lake, to define R_{0m}. These conditions also defined the model cavitation index, σ_{im}. Using Equation 7.15, for an assumed G factor of 1, the full-scale inception index, σ_{if} and depths were determined for the same speed. The bubble radius, R_{0f} at these depths were obtained from the measurement data base in full-scale water body to calculate R_{0m}/R_{0f}, then G factor was determined from Figure 7.3 by interpolation at this R_{0m}/R_{0f} and initial bubble size R_{0m} measured in the lake. If the G factor was sufficiently close to 1.0, the actual value was used for the final value of the full-scale inception index, σ_{if} and depth. If G was significantly different 1.0, then using the R_{0f} values at the new inception depth the ratio of R_{0m}/R_{0f} was re-calculated and G was determined. This procedure is iterated until the solutions are similar.

Based upon the above investigation, Gowing & Shen (2001) concluded that the dynamic range of the nuclei size ratios, R_{0m}/R_{0f}, measured in the test lake and oceans was small. The change in inception index caused only by the nuclei effects was in the order of a few percent. The effect of nuclei variations for the measured data showed small variations from one natural water body to another, but these results may be different at shallower or deeper depths or different times of year. Also, this finding may not be true for scaling water tunnel tests to full-scale environments since the nuclei size ratios could vary much more than the ratios quoted in their paper.

7.3. Review of Keller's Scaling Equation for Cavitation Inception

Keller has been conducting numerous cavitation tests with various types of submerged bodies in VW Obernach at Munich University of Technology since the 1980's. The bodies investigated by Keller, some of which were geosims, varied from axisymmetric forms with hemispherical, conical, ogival, blunt and Schibe heads to various forms of 3-D and 2-D NACA foils section tested at systematically varying angles of attack.

Based upon his investigations, Keller proposed that the cavitation inception number σ_i can be written as independent of the water quality effects, by replacing vapor pressure, Pv by the actual critical pressure for rupture of the liquid as shown in Equation (7.3) in section 7.2.2 He uses a "Vortex Nozzle chamber Technique" as a cavitation susceptibility meter to be used routinely to measure the tensile strength throughout the testing program (Keller (1981)).

Removing the flow tensile strength effect by keeping its value at zero for all tests, Keller investigated the scale effects associated with the flow velocity, body size, viscosity of the fluid and the free stream turbulence during the last decade through numerous systematic tests with the above mentioned submerged test bodies as show in Figure 7.4.

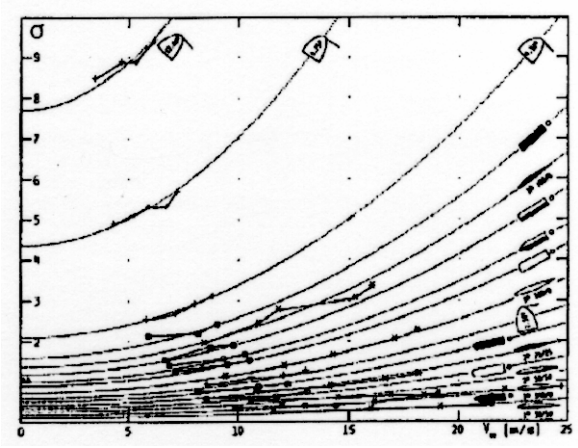

Figure 7.4 Cavitation number – velocity relation for cavitation inception for all body types in liquids of zero tensile strength, Keller (1994).

Based upon his investigations he established an universal empirical scaling relation for incipient cavitation. The derived formula is given as follows, (Keller, 1994).

$$\sigma_i = K\left(\frac{L}{L_0}\right)^{1/2}\left(\frac{\nu}{\nu_0}\right)^{1/4}\left[1+\left(\frac{V}{V_0}\right)^2\right]\left[1+K_0\frac{S}{S_0}\right] \tag{7.16}$$

where L, ν, V and S are the characteristic length of the body, the kinematic viscosity, the free stream velocity, and the turbulence level of the free stream velocity. L_0, ν_0, V_0 and S_0 are reference values. K_0 is an empirical constant which is a characteristic of the body shape and type of cavitation. V_0 is nearly constant which was approximately 12m/s for all the experiments he conducted.

It is important to note that the above relationship is not derived from first principles but is, instead, the best fit to a set of experimental data. This will make extrapolation of the relationship outside of the experimentally derived range very problematic, as discussed below. It also leads to a curious property of the relationship with varying Reynolds number. It is possible to achieve a given Reynolds number both by variation in size and in speed.

For a given value of water quality, one would expect that the inception value would not change with Reynolds number. This is implicit in the assumption that the physical processes for water quality scaling effects can be accounted for by the measurement of the critical pressure alone and its inclusion in the inception index). The viscous scale effects are then accounted for by the right-hand-side of the equation and should be a function of Reynolds number alone (for given freestream turbulence conditions). If the Reynolds number is doubled, with a doubling of the length scale with all else held constant, the predicted inception index from Keller's relationship will increase by a factor of $\sqrt{2}$. But, if the Reynolds number is increased through an increase in the velocity by a factor of 2 with all else constant, the predicted inception value will be quite different, depending in the choice of the parameter V_0. This feature of the relationship is inconsistent with basic similarity ideas of fluid mechanics.

The coefficients of Equation (7.16) are predominantly based on tests with geometrically similar families of rotationally symmetric test bodies of different shapes, the shapes varying from streamlined to blunt, etc. Cavitation inception on such bodies is governed by the pressure distribution on the body surface and the accompanied features of boundary layer flow. On the other hand the inception of tip vortex cavitation depends on the pressure in the center of a free vortex. So, he investigated the validity of the Equation (7.16) for the inception of tip vortex cavitation using four geometrically similar elliptical hydrofoils having outline of 3-D NACA 16020 sections. He showed that Equation (7.16) can be applied to inception of tip vortex cavitation by adding α^2 or $C_L{}^2$, where α is the angle of attack and C_L is the lift coefficient, as shown in Figure 7.5. Also, Keller represented σ_i against Reynolds number based on the classical McCormick (1962) Formula, given by equation (7.1). Keller chose m = 0.5 and showed that the scattering of data is very small as shown in Figure 7.6.

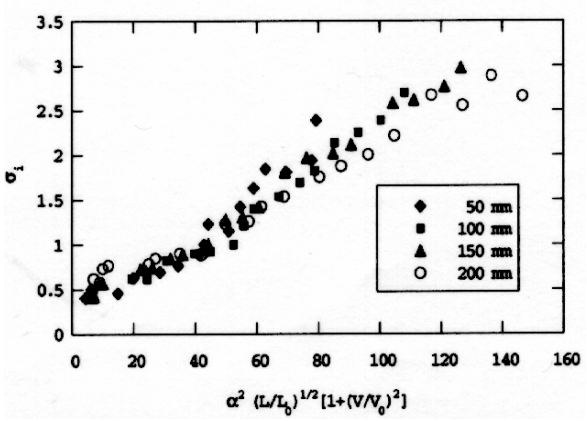

Figure 7.5 Critical cavitation number, σ_i, as a function of $\alpha^2(L/L_0)^{1/2}$ $[1+(V/V_0)^2]$, Keller (2000).

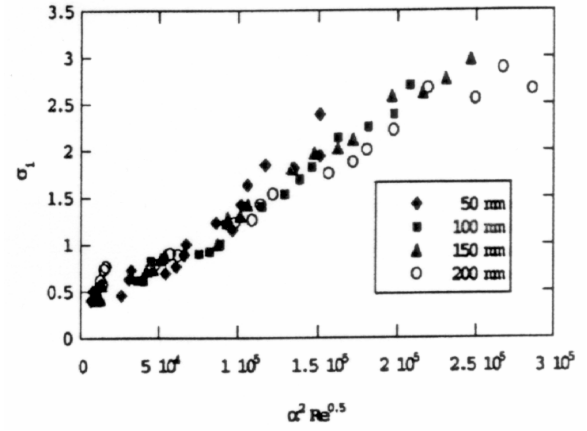

Figure 7.6 Critical cavitation number, σ_i, as a function of $\alpha^2 \mathrm{Re}^{0.5}$, Keller (2000).

Thus, Keller claimed that the equation (7.16) is universal for the inception of various types of cavitation such as bubble, vortex and surface cavitation. However, this claim is open to questions based on the following grounds:

- To correct the viscous effect, Keller eliminates the water quality effect by using "Vortex Nozzle chamber". This type of flow meter is inherently prone to liquid quality effects. Therefore, the entire data may have this effect included.
- Vortex and surface type of cavitation follows different physics. Equation (7.16) has a strong length scale dependency for surface cavitation and it is in contradiction by most experimental data.

- Equation (7.16) is an empirical formula and has no physical basis.

With regard to the final point above, the data on the inception of tip vortex cavitation is considered. Many researchers proposed that m = 0.4 for the exponential of *Re*, based on the flow field measurements near the tip vortex not in model scale but also in full scale (Fruman (1994) Shen et al (2001)). In Figure 7.7, σ_i plotted against $\alpha^2 Re^{0.4}$ instead of $\alpha^2 Re^{0.5}$. The scattering of data is also small as in the case of Figure 7.6. In Figure 7.8, σ_i of another foil section (NACA 4215) plotted against *Re* and the data are fitted for $Re^{0.4}$ and $Re^{0.5}$. The scattering of data is also small both for $Re^{0.4}$ and $Re^{0.5}$.

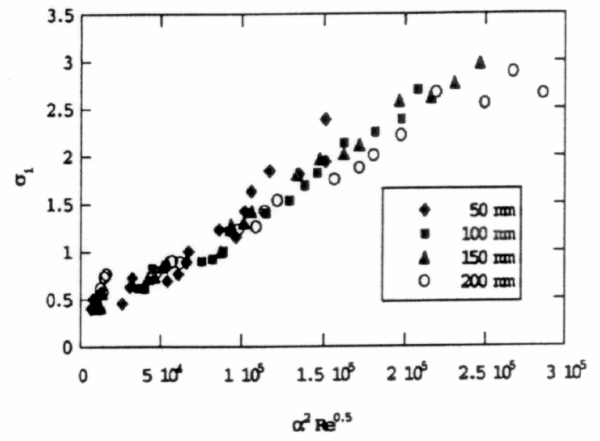

Figure 7.7 Critical cavitation number, σ_i, as a function of $\alpha^2 Re^{0.4}$.

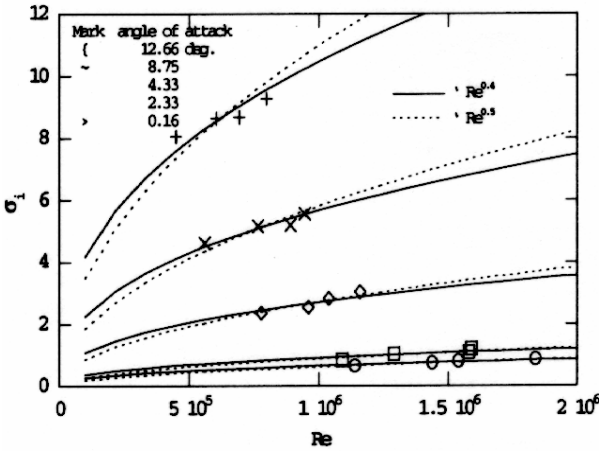

Figure 7.8 Critical cavitation number, σ_i as a function of *Re* for NACA 4215 foil section.

Next, consideration has given to the estimation of full-scale inception from model data. In the case of the ship, the scale ratio of the full scale to the model is 10 times or more. On the other hand, the speed is not much different both in full and model scale. Therefore, Reynolds number in full scale is ten times or more than that in model scale. In Figure 7.9, the data in Figure 7.8 are plotted again for the larger range of Reynolds number. It is obvious that the estimated σ_i using $Re^{0.5}$ is larger than that using $Re^{0.4}$ in full scale Reynolds number (i.e., $>10^7$). So, it is necessary to be careful in using equation (7.16) to estimate the full-scale inception form model data or in other words to extrapolate from the model data. Further investigation is required.

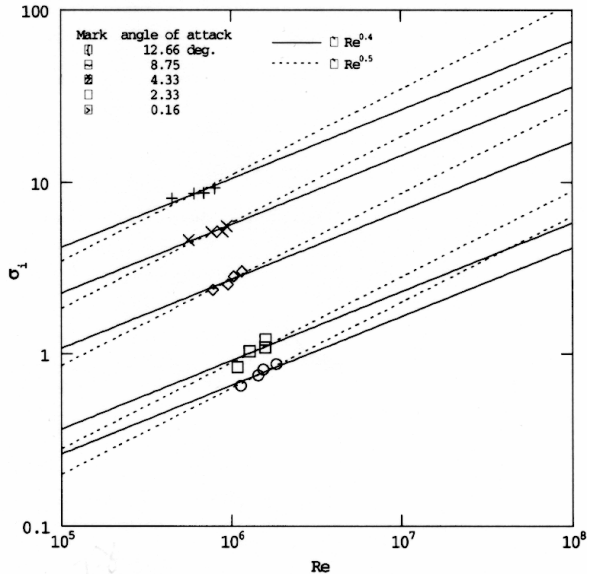

Figure 7.9 Critical cavitation number, σ_i as a function of *Re* (NACA 4215).

7.4. Review of Fresh Water Versus Salt Water Nuclei Effects

Shen et al. (1994) conducted a series of cavitation tests in a water tunnel using both fresh water and salt water. The following summarizes some of the results:

- Salt water had no significant effect on the inception of leading edge sheet cavitation,

- Salt water clouds were more intense and persisted longer than in fresh water
- Salt water microbubbles were more numerous, smaller and persisted for longer times, and
- Fresh water microbubbles were less, larger and disappeared in a relatively short time.

These results support the effect of inorganic salts to change nuclei populations in seawater and results in the foaming that has been observed. It could be concluded that the effect of seawater on cavitation is to shift the nuclei content to smaller and more numerous microbubbles.

8. REPORT SUMMARY

Many observations have been discussed on the effect of water quality on cavitation inception. The following is a brief summary:

1. Cavitation inception criteria are very different between facilities and can be a source of discrepancies and different scaling laws.
2. Water quality effects are related to the water microbubble distribution.
3. Intermittent cavitation is due primarily to microbubble availability at a critical location in a time dependent flowfield.
4. Each testing facility has a unique relationship between the microbubble distribution and the dissolved air content, which depends upon operating conditions (pressure/velocity).
5. Propeller cavitation inception data indicates that water quality has little effect on sheet cavitation but significantly affects bubble and vortex cavitation.
6. Model propeller cavitation experiments can have both water quality and viscous effects. It is important to account for water quality effects before scaling.
7. Water quality effects are minimized at full-scale conditions due to the large scale, higher velocities and sufficient microbubble distribution.

9. CONCLUSION

1. Cavitation nuclei distributions significantly affect cavitation intermittency for all types of cavitation and cavitation inception for bubble and vortex type cavitation.
2. It is recommended that some knowledge of water quality (*liquid tension/nuclei distribution) be known for a cavitation test facility during typical testing conditions.
3. It is recommended that efforts be made to correct cavitation inception data based on liquid vapor pressure for water quality effect. No correction is necessary for sheet cavitation inception. Corrections are necessary for vortex and bubble type of cavitation.
4. It is recommended that some measure/criteria of intermittency at cavitation inception be documented.

10. REFERENCES

Acosta, A.J., and Parkin, B.R., 1974, "Cavitation Inception – A Selective Review", Proc. 17th American Towing Tank Conference, Pasadena, CA, USA (also: Journal of Ship Research, Vol. 19, 193-295, 1975).

Arakeri, V.H., and Acosta, A.J., 1973, "Viscous Effects in Inception of Cavitation on Axisymmetric Bodies", ASME Journal of Fluids Engineering, Vol. 95, pp. 519-527.

Arndt, R.E.A., and Maines, B.H., 1994, "Vortex Cavitation: a Progress Report", ASME FED, Vol. 190, Lake Tahoe, NV, USA.

Billet, M.L., 1986, "The Importance and Measurement of Cavitation Nuclei", Advances in Aerodynamics, Fluid Mechanics and Hydraulics, ASCE, Minneapolis, MN, USA.

Bongiovanni, C., Cheraillier, J.P., and Fabre, J., 1997, "Sizing of Bubbles by Incoherent Imaging: Defocus Bias", Experiments in Fluids, Vol. 23.

Briançon-Marjollet, L., and Merle, L., 1996, "Inception, Development, and Noise of a Tip Vortex Cavitation", 21st Symposium on Naval Hydrodynamics, Trondheim, Norway.

Ceccio, S.L., and Brennen, C.E., 1992, "Observations of the Dynamics and Acoustics of Traveling Bubble Cavitation", Journal Fluid Mechanics, Vol. 233.

Ceccio, S.L., Gowing, S., and Shen, Y., 1997, "The Effects of Salt Water on Bubble Cavitation", ASME Journal Fluids Engineering, Vol. 119, No. 1, pp. 155-163.

Ceccio, S.L., Judge, C., Fry, D., Chesnakas, C., Jessup, S., and Oweis, G.F., 2001a, "Cavitation Inception in Tip leakage Vortices", CAV 2001 – 4th International Symposium on Cavitation, Pasadena, CA, USA.

Ceccio, S.L., Judge, C., Fry, D., Chesnakas, C., Jessup, S., Oweis, G.F., 200lb, "PIV Measurement of a Tip Leakage Vortex", Proc. 26th American Towing Tank Conference, Glen Cove, NY, USA.

d'Agostino, L., and Acosta, A.J., 1991, "A Cavitation, Susceptibility Meter With Optical Cavitation Monitoring", ASME Journal of Fluids Engineering, Vol. 113, No. 2, pp. 261-269.

Frechou, D., Dugué, C., Briançon-Marjollet, L., Fournier, P., Darquier, M., Descotte, L., and Merle, L., 2000, "Marine Propulsor Noise Investigation in the Hydroacoustic Water Tunnel", 23rd Symposium on Naval Hydrodynamics, Val de Reuil, France.

Friesch, J., 2000, "Ten Years of Research in Hydrodynamics and Cavitation Tunnel-HYKAT of HSVA", NCT'50 International Conference of Propeller Cavitation, Newcastle upon Tyne, United Kingdom.

Fruman, D.H., Dugué, C., and Cerrutti, P., 1991, "Tip vortex Roll-up and Cavitation", ASME FED, Vol. 109.

Fruman, D.H., 1994, "Recent Progress on the Understanding and Prediction of Tip Vortex cavitation", 2nd International Symposium on Cavitation, Tokyo, Japan.

Fruman, D.H., Cerruti, P., Pichon, T., and Dupont, P., 1995, "Effect of Hydrofoil Planform on Tip Vortex Roll-Up and Cavitation", ASME Journal of Fluids Engineering, Vol. 117.

Gates, E.M., and Bacon, J., 1978, "A Note on the Determination of Cavitation Nuclei Distribution by Holography", Journal of Ship Research, Vol. 22.

Gates, E.M., and Billet, M.L., 1980, "Cavitation Nuclei and Inception", IAHR Symposium, Tokyo, Japan.

Gindroz, B., and Billet, M.L., 1994a, "Nuclei and Acoustic Cavitation Inception on Ship Propellers", 2nd International Symposium on Cavitation, Tokyo, Japan.

Gindroz, B., and Billet, M.L., 1994b, "Nuclei and Propellers Cavitation Inception", Proc. ASME FED Symposium on Cavitation, Lake Tahoe, NV, USA.

Gindroz, B., 1995, "Propeller Cavitation Characteristics: The Practical Interest of Nuclei Measurements in Test Facilities and At Sea", ASME FED, Vol. 226, Hilton Head, SC, USA.

Gindroz, B., and Matera, F., 1996, "Influence of the Cavitation Nuclei on the Cavitation Bucket When Predicting the Full-Scale Behavior of a Marine Propeller", 21st Symposium on Naval Hydrodynamics, Trondheim, Norway.

Gindroz, B., and Billet, M.L., 1998, "Influence of the Nuclei on the Cavitation Inception for Different Types of Cavitation on Ship Propellers", ASME Journal of

Fluids Engineering, Vol. 120, pp. 171-178.

Gowing, S., and Shen, Y., 2001, "Nuclei Effects on Tip Vortex Cavitation Scaling, CAV 2001 – 4th International Symposium on Cavitation, Pasadena, CA, USA.

Holl, J.W., Arndt, R.E.A., Billet, M.L., 1972, "Limited Cavitation and the Related Scale Effects Problem", Proc. 2nd Int. Symp. Fluid Mech. Fluidics, JSME, Tokyo, pp. 303-314.

ITTC, 1990, "Report of the Cavitation Committee", Proc. 19th International Towing Tank Conference, Vol. I, Madrid, Spain.

ITTC, 1993, "Report of the Cavitation Committee, Proc. 20th International Towing Tank Conference, Vol I, San Francisco, CA, USA.

ITTC, 1996, "Report of the Cavitation Committee", Proc. 21st International Towing Tank Conference, Vol. I, Trondheim, Norway.

Kates, J., 1978, "Determination of Solid Nuclei and bubble Distribution I Water by Holography", Report No. Eng. 183-3, California Institute of Technology, Pasadena, CA, USA.

Keller, A.P., 1994, "New Scaling Laws for Hydrodynamic Cavitation Inception", 2nd. International Symposium on Cavitation, Tokyo, Japan.

Keller, A.P., 2000, "Cavitation Scale Effects, a Representative of its Visual Appearance and Empirically Found Relations", NCT'50 International Conference of Propeller Cavitation, Newcastle Upon Tyne, United Kingdom.

Keller, A.P., 1981, "Tensile Strength of Liquids", Proc. 5th International Symposium on Water Column Separation, IAHR Work Group, Obernach, Germany.

Korkut, E., and Atlar, M., 2001, "On the Importance of the Effect of Turbulence in Cavitation Inception Tests of Marine propellers", Proc. Royal Soc. London A (2002), 458.

Maxey, M.R., and Riley, J.J., 1983, "Equation of Motion for a Small Rigid Sphere in Nonuniform Flow", Physics of Fluids, Vol. 26.

McCormick, B.W., 1962, "On Cavitation Produced by a Vortex Trailing From a Lifting Surface", ASME Journal of Basic Engineering, Vol. 84, pp. 269-279.

Pauchet, A, Briançon-Marjollet, L., Gowing, S., Cerrutti, P. and Pichon, T., 1994, "Effects of Foil Size and Shape on Tip Vortex Cavitation Occurrence", 2nd International Symposium on Cavitation, Tokyo, Japan.

Plesset, M.S., 1948, "Dynamics of Cavitation Bubbles", Journal of Applied Mechanics, Vol. 16.

Semionicheva, E.Ya., and Startsev, S.B., 2001, "Multi-Point Profiles of Hydrofoils and Propulsor Blades in Nonuniform Flow", MARIND 2001 – Third International Conference on Marine Industry, Varna, Bulgaria.

Shen, Y.T., Chahine, G., Hsiao, C.T., and Jessup, S., 2001, "Effects of Model Size and Free Stream Nuclei on Tip Vortex Cavitation Scaling", CAV 2001 – 4th International Symposium on Cavitation, Pasadena, CA, USA.

Shen, Y.T., Gowing, S., and Ceccio, S., 1994, "Salt Water Effects on bubble and sheet Cavitation", 2nd International Symposium on Cavitation, Tokyo, Japan.

Tanger, H., and Weitendorf, E.A., 1989, "Applicability Tests for the Phase Doppler Anemometer for Cavitation nuclei measurement", ASME International Symposium on Cavitation Inception, San Francisco, CA, USA.

The Specialist Committee on Water Quality and Cavitation

Committee Chair: Dr. Michael Billet (ARL-PSU)
Session Chair: Prof. Hiroharu Kato (Toyo University)

I. DISCUSSIONS

I.1. Discussion on the Report of the 23rd ITTC Specialist Committee on Water Quality and Cavitation: Minimum equipment necessary to a new cavitation tunnel

By: Neil Bose, Memorial University of Newfoundland, Canada

If one wants to build a new cavitation tunnel, what would the Committee consider to be the minimum equipment necessary to carry out useful and worthwhile tests?

What equipment would be needed to measure the water quality and what equipment would be needed to control the water quality (gas content, nuclei distribution, etc.)?

I.2. Discussion on the Report of the 23rd ITTC Specialist Committee on Water Quality and Cavitation: Importance of the flow history in cavitation inception

By: Thomas J.C. van Terwisga, MARIN, The Netherlands

The Committee made it clear that both the facility and the operating conditions of the facility, including the total air content, do have an effect on the nuclei density spectrum.

Furthermore the Committee states that the flow history has an effect on the nuclei density spectrum.

Could the Committee indicate how important the flow history is in, e.g., cavitation inception tests? And, if important, which method would be most suitable to measure the nuclei density spectrum during the testing period in a practical and cost efficient way?

I.3. Discussion on the Report of the 23rd ITTC Specialist Committee on Water Quality and Cavitation: Control of water quality in cavitation tunnel

By: Hiraku Kamiirisa, Mitsui Akishima Laboratory, Japan

Concerning the control of water quality in cavitation tunnel, extensive researches have been made in our laboratory so far. I would like to discuss some issues in controlling nuclei in the tunnel showing some typical measurements in our laboratory.

Nuclei measuring device

From the viewpoint of the practical nuclei control, it is required that the nuclei measuring device is rather low-cost one with appropriate accuracy and quick response.

We measured bubble nuclei distribution by the light-extinction device which is more convinient than other device. It was found that the measured nuclei distribution was different by the water tube sampler length as shown in Figure I.3.1.

An arrangement of the device is shown in Figure I.3.3 and the light-extinction nuclei measuring device is shown in Figure I.3.4.

In related to this problem, we will develop the optimum nuclei measuring device for nuclei control in the future.

Nuclei control method

For the purpose of the nuclei control, we put the micro bubble (the 20 micron peak) into the cavitation tunnel, and measured the nuclei distribution.

The nuclei size increased gradually as shown in Figure I.3.2. We found that this might be caused by the coalescence during the bubble circulating in the tunnel. Simulation study is now being made extensively in order to investigate its cause and develop a practical nuclei control method.

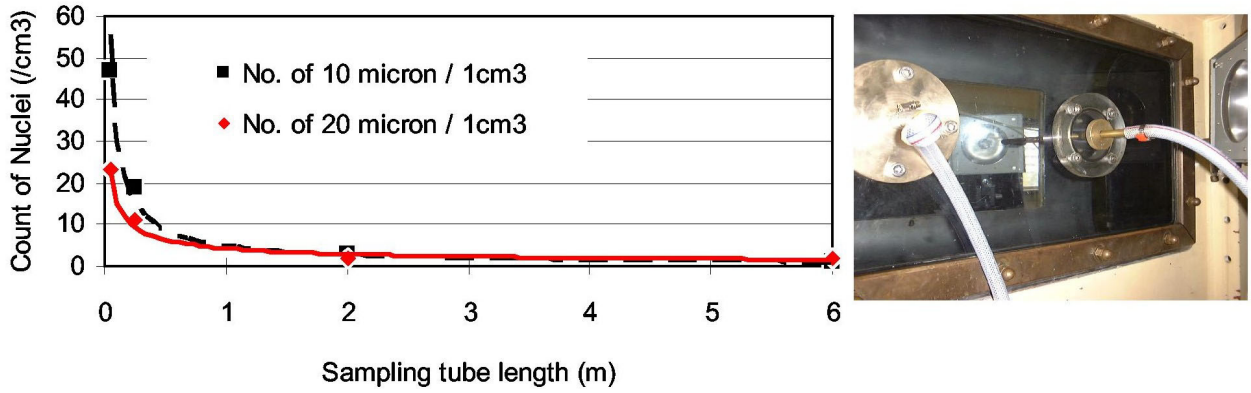

Figure I.3.1 Effect of sampling tube length on nuclei measurement by light-exctinction method.

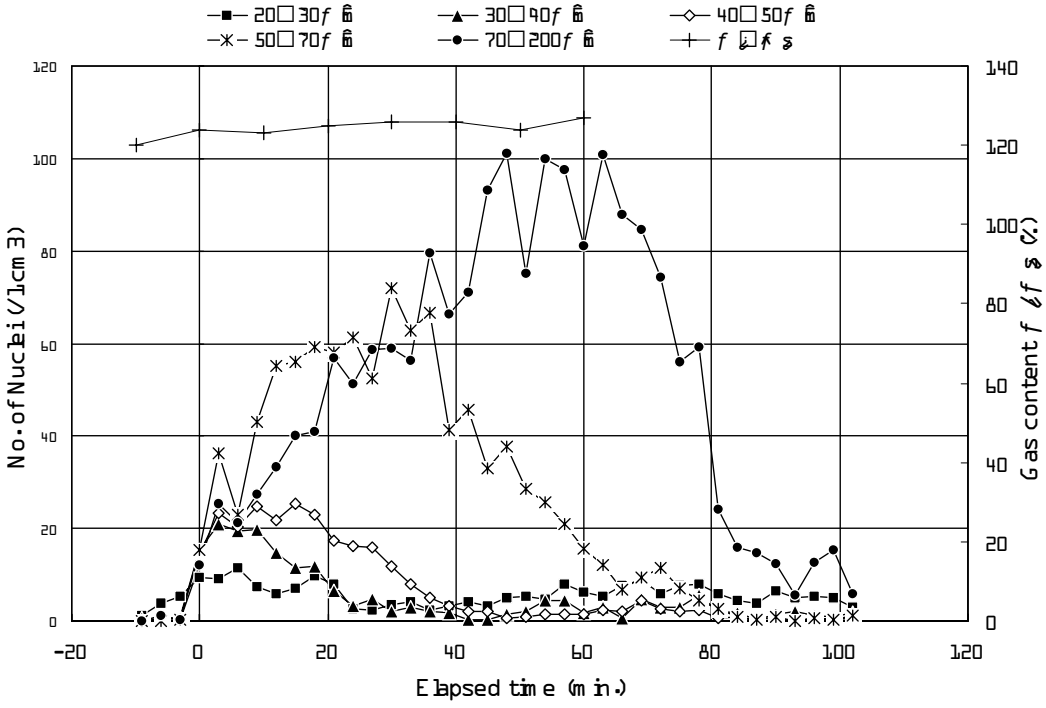

Figure I.3.2 Nuclei distribution by micro bubble injection (initial: 0.1056 MPA, 4.0 m/s, Gas content: 120%).

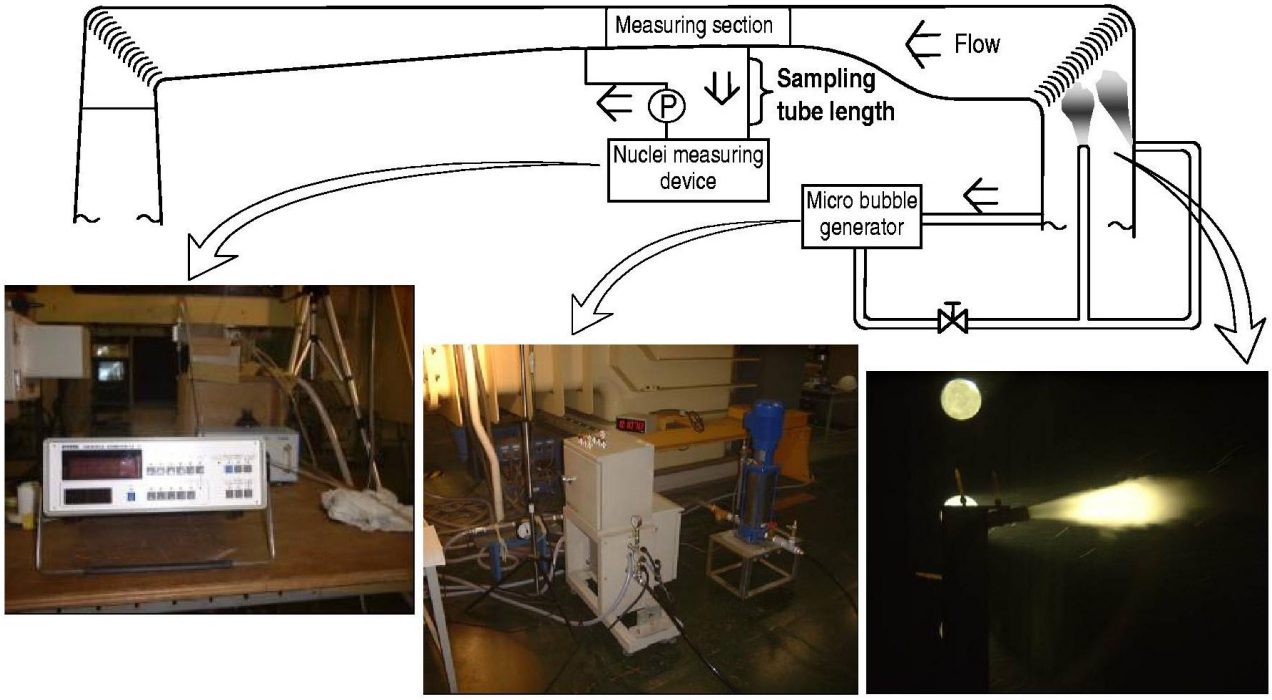

Figure I.3.3 Arrangement of nuclei measuring device and micro bubble generator.

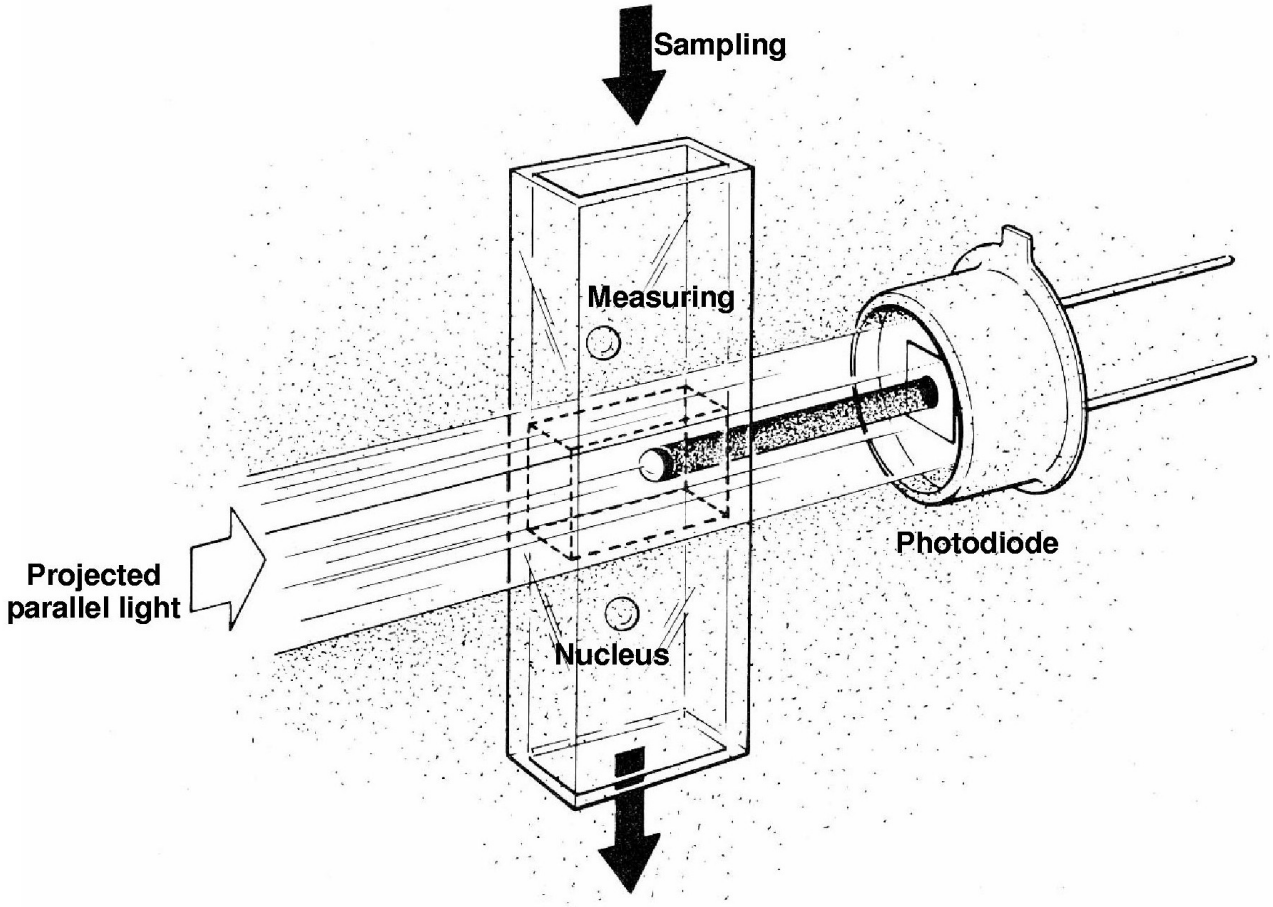

Figure I.3.4 Conceptual sensor structure of light extinction nuclei measuring device.

II. COMMITTEE REPLIES

II.1. Reply of the 23rd ITTC Specialist Committee on Water Quality and Cavitation to Neil Bose

The Committee strongly recommends that some knowledge of water quality is necessary for each facility. The influence of nuclei size and concentration for both cavitation inception and cavitation patterns is well documented. It is not necessary, however, to measure the nuclei concentration liquid tension during each test.

A summary of different devices is given in the report. A device that measures the free gas/oxygen content represents some knowledge, but is not sufficient. A device that measures liquid quality has been shown to correlate most water quality effects. However, cavitation studies in water tunnels require a device that measures both nuclei size and distribution.

II.2. Reply of the 23rd ITTC Specialist Committee on Water Quality and Cavitation to T.J.C. van Terwisga

First of all, the Committee agrees with Dr. Tom van Terwisga that it is very important to quantify the effect of flow history on water quality effects. This is a very difficult question to answer because each facility is different, and this has led to much discussion by the Committee. One example is given in Section 5.4 documenting the propeller cavitation tests conducted at CEIMM facility. As the velocity is increased, the absolute pressure at inception increases. As the pressure is changed, so is the nuclei distribution. An estimated effect is in the order of 10% for a given oxygen content.

The report summarizes several measuring techniques. It is important for each facility to determine which measurement device is most practical and cost effective for the types of experiments conducted.

II.3. Reply of the 23rd ITTC Specialist Committee on Water Quality and Cavitation to H. Kamiirisa

The Committee is encouraged to hear the nuclei measurement and control activities reported in this contribution and would be pleased to make comments on these activities.

As far as the nuclei measurements activities are concerned, one of the recommendations of this Committee is to have some knowledge of water quality for any cavitation testing facility. The Committee therefore encourages these measurements. Several papers reported in the committee report, particularly those compare different measuring devices could be relevant to the contributor to compare their proposed device. It is also recommended to do these measurements as close as possible to the testing section.

As far as the nuclei control activities are concerned, as it is underlined in the Committee report, the nuclei content is strongly connected to the facility. The Committee also emphasises to the following points:

- A high level of oxygen content results in an increase of bubble size with time and in vaporous cavitation;
- The recirculation of nuclei can be important and must be taken into account during test procedure.

The Committee also notes the large concentration of nuclei used in this study. It is not necessary to reach such high concentration to reduce the effect of water quality as it can be observed on different figures in the Committee report.